Chemical Research in Toxicology

pubs.acs.org/crt

Article

Cystine/Glutamate Xc⁻ Antiporter Induction Compensates for Transsulfuration Pathway Repression by 2,3,7,8-Tetrachlorodibenzo-*p*-dioxin (TCDD) to Ensure Cysteine for Hepatic Glutathione Biosynthesis

Karina Orlowska, Russ R. Fling, Rance Nault, Anthony L. Schilmiller, and Timothy R. Zacharewski*

Cite This: *Chem. Res. Toxicol.* 2023, 36, 900−915

Read Online

ACCESS | Metrics & More | Article Recommendations | Supporting Information

ABSTRACT: Exposure to 2,3,7,8-tetrachlorodibenzo-*p*-dioxin (TCDD) has been associated with the induction of oxidative stress and the progression of steatosis to steatohepatitis with fibrosis. It also disrupts metabolic pathways including one-carbon metabolism (OCM) and the transsulfuration pathway with possible consequences on glutathione (GSH) levels. In this study, complementary RNAseq and metabolomics data were integrated to examine the hepatic transsulfuration pathway and glutathione biosynthesis in mice following treatment with TCDD every 4 days for 28 days. TCDD dose-dependently repressed hepatic cystathionine *β*-synthase (CBS) and cystathionine *γ*-lyase (CTH) mRNA and protein levels. Reduced CBS and CTH levels are also correlated with dose-dependent decreases in hepatic extract hydrogen sulfide (H_2S). In contrast, cysteine levels increased consistent with the induction of *Slc7a11*, which encodes for the cystine/glutamate Xc⁻ antiporter. Cotreatment of primary hepatocytes with sulfasalazine, a cystine/glutamate Xc⁻ antiporter inhibitor, decreased labeled cysteine incorporation into GSH with a corresponding increase in TCDD cytotoxicity. Although reduced and oxidized GSH levels were unchanged following treatment due to the induction of GSH/GSSG efflux transporter by TCDD, the GSH:GSSG ratio decreased and global protein S-glutathionylation levels in liver extracts increased in response to oxidative stress along with the induction of glutamate-cysteine ligase catalytic subunit (*Gclc*), glutathione synthetase (*Gss*), glutathione disulfide reductase (*Gsr*), and glutathione transferase *π* (*Gstp*). Furthermore, levels of ophthalmic acid, a biomarker of oxidative stress indicating GSH consumption, were also increased. Collectively, the data suggest that increased cystine transport due to cystine/glutamate Xc⁻ antiporter induction compensated for decreased cysteine production following repression of the transsulfuration pathway to support GSH synthesis in response to TCDD-induced oxidative stress.

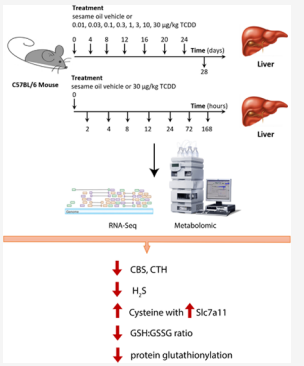

INTRODUCTION

Inappropriate management of oxidative stress can lead to hepatotoxicity and contribute to adverse outcomes such as liver disease including non-alcoholic fatty liver disease (NAFLD) and hepatocellular carcinoma (HCC). In response, highly conserved defense systems have evolved to ensure redox balance and cell homeostasis are maintained. Antioxidant defense systems such as reduced glutathione (GSH) scavenge reactive oxygen species (ROS) to protect macromolecules from damage and ensure cell viability.[1] The antioxidant properties of GSH are largely due to the reduction of hydrogen and lipid peroxides by GSH peroxidases (GPX) resulting in the formation of glutathione disulfide (GSSG), which can be recycled to GSH by glutathione reductase at the expense of reduced nicotinamide adenine dinucleotide phosphate (NADPH) under normal conditions.[2] In addition to serving as a direct free radical scavenger and a sink for cysteine, GSH can be conjugated to electrophilic intermediates by glutathione *S*-transferases to facilitate detoxification and excretion.[3,4] GSH is also a substrate for the post-translational modification of proteins.[5] Protein S-glutathionylation can be transient or persistent after sulfhydryl oxidation through intermediate moieties such as sulfenic acid. In general, S-glutathionylation increases with oxidative stress to protect protein thiol groups from irreversible oxidation and also has roles in cell signaling and regulating protein function.[5] Therefore, oxidative stress is more than just an imbalance between ROS production and endogenous antioxidant scavenging capacity resulting in ROS accumulation but a consequence of an imbalance between redox signaling and control mechanisms.[6]

GSH is the most abundant cellular nonprotein thiol in eukaryotic organisms from yeast to humans with millimolar levels present in the liver.[2] This ubiquitous tripeptide containing glutamate, glycine, and cysteine is synthesized in the cytosol using a nonribosomal pathway involving two

Received: January 26, 2023
Published: May 15, 2023

adenosine 5′-triphosphate (ATP)-dependent enzymes. The first, and rate-limiting reaction, synthesizes L-glutamyl-cysteine using glutamate and cysteine, catalyzed by glutamate-cysteine ligase (GCL). Glutathione synthetase (GSS) then ligates glycine to L-glutamyl-cysteine to yield GSH. In addition to GCL activity, GSH levels are regulated by cysteine availability, GSH feedback inhibition, and GSH export.[7] Nearly all plasma GSH is synthesized in the liver, and therefore disruption of hepatic GSH synthesis can impact systemic redox balance.[2]

Cysteine dependence links GSH biosynthesis to the methionine cycle/one-carbon metabolism (OCM), transsulfuration pathway, folate cycle, and bile acid biosynthesis. OCM reversibly converts methionine to homocysteine, which can be irreversibly metabolized to cysteine via the transsulfuration pathway. Approximately half of the cysteine produced by transsulfuration is used to support hepatic GSH biosynthesis.[8,9] However, cysteine can also be metabolized into taurine with possible conjugation to cholic acid to provide various bile acids.[10] Moreover, cysteine is a metabolic source of sulfate and hydrogen sulfide (H_2S), an important endogenous cellular gaseous signal mediator that directly modulates downstream targets. Consequently, the highly regulated transsulfuration pathway sits at the intersection of several pathways with its disruption associated with various diseases including NAFLD and HCC.[11,12]

Several endogenous and exogenous factors influence GSH biosynthesis. This includes diverse halogenated aromatic hydrocarbons (HAHs) that induce xenobiotic (i.e., cytochrome P450 activity) and purine (i.e., XDH/XO) metabolizing enzymes that produce ROS as well as the conversion of methionine to cysteine to support increased GSH synthesis.[13,14] 2,3,7,8-Tetrachlorodibenzo-*p*-dioxin (TCDD) belongs to a class of persistent environmental contaminants that includes polychlorinated dioxins (PCDDs), dibenzofurans (PCDFs), and biphenyls (PCBs). TCDD induces biochemical and toxic effects via the aryl hydrocarbon receptor (AhR), a promiscuous ligand-activated basic helix-loop-helix PER-ARNT-SIM transcription factor. Diverse chemicals, endogenous metabolites, microbial products, and dietary constituents bind and activate the AhR.[15,16] Following ligand binding, the activated AhR translocates to the nucleus where it forms a heterodimer with the AhR nuclear translocator (ARNT). The AhR−ARNT complex regulates gene expression by interacting with response elements containing the 5′-GCGTG-3′ core sequence as well as nonconsensus sites throughout genome recruiting coactivators to elicit changes in gene expression resulting in toxicity.[16,17] This includes the induction of genes associated with hepatic fat accumulation and enzyme activities known to produce ROS that contribute to TCDD and related compound hepatotoxicity.[18−20]

Studies have also shown that TCDD and other contaminants dose-dependently induce the progression of steatosis to steatohepatitis with fibrosis in mice.[21−23] This was accompanied by the reprograming of central carbon metabolism and the induction of pyruvate kinase muscle isoform 2 (PKM2), which is typically associated with the Warburg effect in cancer cells.[24,25] PKM2 expression can reduce glycolytic flux and redirect accumulating upstream intermediates to serine/glycine biosynthesis and the pentose phosphate pathway to provide intermediates in support of GSH biosynthesis and reducing equivalents for oxidized GSH (GSSG) recycling. TCDD also disrupts OCM, which feeds homocysteine into the transsulfuration pathway to synthesize cysteine for GSH synthesis.[26]

This study further examined the hypothesis that OCM disruption by TCDD impairs the transsulfuration pathway with consequences for GSH biosynthesis and TCDD toxicity. The integration of complementary RNAseq and metabolomics data with tracer studies in primary hepatocytes showed that despite the induction of cystine/glutamate transport to compensate for the transsulfuration pathway repression, the GSH/GSSG ratio decreased consistent with TCDD-induced oxidative stress and protein glutathionylation.

MATERIALS AND METHODS

Animal Treatment. Male C57BL/6 mice were obtained from Charles River Laboratories (Kingston, NY). Animals weighing within 10% of each other were housed in Innovive Innocages (San Diego, CA) with ALPHA-dri bedding (Shepherd Specialty Papers, Chicago, IL) in a 12/12 h light/dark cycle and 23 °C environment with 30−40% humidity. The mice had ad libitum access to food (Harlan Teklad 22/5 Rodent Diet 8940, Madison, WI) and Aquavive water (Innovive). On postnatal day (PND) 28, at the start of the light cycle (zeitgeber time [ZT] 0−1), the mice were gavaged with 0.1 ml sesame oil vehicle (Sigma-Aldrich, St. Louis, MO) or 0.01, 0.03, 0.1, 0.3, 1, 3, 10, and 30 μg/kg body weight TCDD (AccuStandard, New Haven, CT). Doses were administered every 4 days for 28 days for a total of seven treatments. The first treatment was executed on day 0 with the final gavage given on day 24 of the 28-day study. On day 28 tissue samples were collected. The doses used in the current study were chosen to account for the relatively short study duration as opposite to lifelong cumulative human exposure from diverse AhR ligands, the bioaccumulative nature of halogenated AhR ligands, and different half-lives of TCDD in humans (1−11 years),[27,28] and mice (8−12 days).[29] The same dose range and treatment regimen has been used in previous studies where we found that mouse hepatic tissue levels were comparable to serum levels following the intentional poisoning of Viktor Yushchenko (30 μg/kg), of Seveso women following accidental exposure from a 1976 chemical plant accident (0.03−0.1 μg/kg), and dioxin-like compound levels in U.S., German, Spanish and British serum samples (0.01 μg/kg).[30−34] All animal procedures were in accordance with the Michigan State University (MSU) Institutional Animal Care and Use Committee (IACUC; PROTO202100219).

Liquid Chromatography−Tandem Mass Spectrometry. GSH, GSSG, and cysteine were isolated and analyzed as previously described with slight modifications.[35] Briefly, frozen liver samples (~25 mg) were homogenized (Polytron PT2100, Kinematica, Lucerne, Switzerland) in methanol containing 50 mM *N*-ethylmaleimide (NEM) and [$^2H_5$]GSH, [$^{13}C_4$,$^{15}N_2$]GSSG (Toronto Chemicals, Canada) as well as [^{13}C, ^{15}N]cysteine (Sigma-Aldrich) as internal standards followed by incubation at room temperature to allow for derivatization of GSH and cysteine thiols with NEM. The supernatant was dried under nitrogen and resuspended in 0.1% aqueous formic acid. GSH-NEM, GSSG, and cysteine-NEM were separated in reversed-phase mode on an Acquity HSS T3 column (1.8 μm, 100 × 2.1 mm^2; Waters, Milford, MA). Solvent A was 0.1% formic acid in water, and solvent B was methanol. The mobile phase gradient was as follows 0 min−100% A, 1.5 min−100% A, 6 min−50% A, 6.01 min−1% A, 7 min−1% A; 7.01−100% A, and 8.5 min−100% A with the flow rate 0.3 mL/min. Mass spectrometry detection was performed using a Xevo G2-XS quadrupole time-of-flight (QTof) by positive electrospray ionization. Compounds were identified based on retention time and mass accuracy using MassLynx Version 4.2 (Waters). To quantify the signals, standard calibration curves were made for each analyzed compound with the six-point curve of serially diluted unlabeled standards with the corresponding labeled internal standards at a constant concentration.

Other compounds were analyzed as previously described.[26] Cystathionine, serine, glycine, glutamate, and 2-aminobutyric acid were extracted from frozen liver samples (~25 mg) using 600 μL of 0.4 M perchloric acid (PCA). To neutralize the solution, 70 μL of

https://doi.org/10.1021/acs.chemrestox.3c00017
Chem. Res. Toxicol. 2023, 36, 900−915

supersaturated potassium bicarbonate ($KHCO_3$) was added. Next, samples were centrifuged (10 min at 13,000*g*) and the supernatant (200 μL) was transferred to 466.67 μL of acetonitrile + 0.1% formic acid making a final 70:30 AcN/H_2O solution with a final dilution of 1:3. Extracts were separated on a Waters Acquity UPLC BEH amide column (1.7 μM particle size, 2.1 × 100 mm^2, Waters) held at 40 °C using Waters UPLC system equipped with a Water TQD triple quadrupole mass spectrometer run in positive ionization mode. The mobile phases were 10 mM ammonium formate + 0.1% formic acid for solvent A and AcN for solvent B. Mobile phase gradient program was as follows: 0 min−1% A, 7 min−50% A, 8 min−50% A, 8.01 min−1% A 10 min−1% A. The flow rate was 0.3 mL/min.

A modified extraction and derivatization protocol was used for ophthalmic acid.[36] Briefly, frozen samples (~25 mg) were homogenized using a metal bead in 600 μL of ice-cold 0.4 M PCA spiked with internal standards.

After centrifugation (13,000*g* for 10 min at 4 °C), 15 μL of the supernatant was derivatized with 6% benzoyl chloride and followed by vortexing every 15 min for 1 h at room temperature. Finally, the samples were reconstituted in potassium hydroxide (2 M, KOH) with 3.2 M formic acid for analysis. Derivatized extracts were separated with a Waters Acquity UPLC BEH C18 column (1.7 μM particle size, 2.1 × 100 mm^2) held at 30 °C using solution A—water + 0.1% formic acid and solution B—AcN. Mobile phase gradient program was as follows: 10% B for 2 min; increased to 90% B from 2 to 10 min; 90% B from 10 to 11 min, and then 10% B from 11 to 13.3 min. The injection volume was 5 μL, and the flow rate was 0.3 mL/min. The QTof was run in positive ionization mode with continuum data acquisition, and leucine enkephalin was used as the lockspray reference compound. The results were normalized to the amount of total protein for each sample. The following internal standards were applied: [$^{13}C_2$,^{15}N]glycine (for cystathione), [$^{13}C_3$,^{15}N]serine (for serine), [$^{13}C_2$,^{15}N]glycine (for glycine), [$^{13}C_5$,$^{15}N_2$]glutamic acid/glycine (for glutamate and ophthalmic acid). Extracts from cells cultured with $^{13}C_3$,^{15}N-cysteine were prepared and analyzed without internal standards. The MRM transitions for TQD triple quadrupole mass spectrometer MS methods and the accurate masses and retention times of compounds analyzed on the QTof are presented in Tables S1 and S2.

Gene Expression, ChIP, pDRE. Genes were considered differentially expressed when |fold-change| ≥ 1.5 and posterior probability values ($P1(t)$) ≥ 0.8 as determined by an empirical Bayes approach.[37] Note that all fold-changes reported and discussed in the text were from diurnal controlled mice treated with 30 μg/kg TCDD every 4 days for 28 days, unless otherwise indicated. Hepatic time course (GSE109863), and dose response (GSE87519) RNAseq gene expression datasets are available at the Gene Expression Omnibus. AhR ChIPseq (GSE97634), NRF2 ChIPseq (GSE109865), and computationally identified putative dioxin response elements (pDREs, https://doi.org/10.7910/DVN/JASCVZ) data were previously published.[17,38,39] Significant AhR ChIPseq binding used a false discovery rate (FDR) ≤ 0.05. pDREs were considered functional with a matrix similarity score (MSS) ≥ 0.856.

Protein Extraction and Western Blotting. Liver samples were homogenized in radioimmunoprecipitation assay (RIPA) buffer supplemented with protease inhibitor cocktail (Sigma). After centrifugation, the total protein concentration was measured in the supernatant fraction using the bicinchoninic acid (BCA) assay (Sigma, St. Louis, MO). Protein samples (20 mg) were resolved by sodium dodecyl sulfate-polyacrylamide gel electrophoresis (SDS-PAGE) in 10% gels (Bio-Rad, San Diego, CA) and transferred to nitrocellulose membranes (GE Healthcare) by wet electroblotting (100 V, 45 min) in the Mini Trans-Blot Cell Unit (BioRad). The membranes were blocked with 5% nonfat milk (in Tris-buffered saline [TBS] + 0.01% Tween) for 1 h and incubated overnight at 4 °C with the following primary antibodies: anti-cystathionine γ-lyase (anti-CTH) (1:1000; ab151769; Abcam, Cambridge, U.K.), anti-cystathionine β-synthase (anti-CBS) (1:2000; 14787-1-AP, Proteintech, Rosemont, IL), anti-GPX2 (1:2000; ab137431; Abcam), and anti-β-actin (1:1000; 4970s; Cell Signaling Technology, Danvers, MA). On the next day, membranes were washed three times with 0.1% TBST at room temperature. To visualize the signal on the membrane, the horseradish peroxidase (HRP)-linked secondary antibodies (1:3000; 7074S; Cell Signaling Technology) and ECL kit (Millipore Corporation, Billerica, MA) were used. Membranes were scanned on a Sapphire Biomolecular Imager (Azure Biosystem, Dublin, CA). Two images were captured for each blot to visualize the chemiluminescence protein product recognized by the antibody, and a second to visualize the molecular weight marker. The images were overlayed to estimate the molecular weight of the visible bands.

Protein density was analyzed using ImageJ software (version 1.47; National Institutes of Health). The expression level of the protein of interest was normalized to β-actin level. For protein glutathionylation analysis, liver samples were homogenized in RIPA buffer supplemented with protease inhibitor cocktail (Sigma) in 20 mM NEM. Protein samples were then separated by nonreducing SDS-PAGE. Samples were subjected to membrane transfer, blocking, incubation with antibodies, and image development as described above, in 10 mM NEM buffer. The antibodies used were anti-glutathione antibody [D8] (ab19534, 1:1000, Abcam) and the horseradish peroxidase (HRP)-linked secondary antibodies (ab6789, 1:5000, Abcam). Row images of western blots used for analysis are presented in Figure S1.

Capillary Electrophoresis. The WES capillary electrophoresis system (ProteinSimple, San Jose, CA) was used following standard manufacturer protocols with the xCT/Slc7a11 antibodies (Cell Signaling, D2M7A) diluted 1:60. An anti-rabbit detection module (ProteinSimple) was used to detect primary antibodies. The intensity of the chemiluminescence signal was analyzed with Compass Software v4.0.0 (ProteinSimple). Representative spectra can be found in Figure S5.

H_2S Measurement. H_2S gas emission was measured using the OxiSelect Free Hydrogen Sulfide Gas Assay Kit (Cell Biolabs, Inc., San Diego, CA) according to manufacturer instructions. Briefly, ~20 mg liver samples were placed in a 96-well microplate. Released H_2S gas was captured in a thin polymer surface containing Ag^+ ions as a brownish-colored silver sulfide spot on the underside of the microplate lid just above the sample. After 1 h, the coated lid was transferred to an empty microplate and optical density (OD) was measured at 405 nm. Serial dilutions of sodium sulfide were used to prepare a standard curve.

Primary Hepatocytes Culture and Treatment. Hepatocytes from male mice (10−11 weeks) were isolated using a two-step perfusion procedure as previously described.[40] Cell aggregates and liver chunks were removed by filtration with cells enrichment by Percoll density centrifugation. Trypan blue exclusion suggested greater than 95% viability. Hepatocytes were plated at a density of 0.5 × 10^6 cells/well in 12-well plates precoated with type I collagen in Williams E medium containing 5% fetal bovine serum (FBS), 1% penicillin/streptomycin, 1% Glutamax, 0.3 mM ascorbic acid, and 100 nM dexamethasone.[41] After 3 h, nonadherent cells were removed, and fresh Williams E medium containing 1% ITS Premix Universal Culture Supplement,[42] 1% penicillin/streptomycin, 1% Glutamax, 0.3 mM ascorbic acid, and 100 nM dexamethasone was replaced. The cells were treated with 0.1 μM to 1 mM sulfasalazine, 10 nM TCDD or vehicle (DMSO) and incubated for 24, 48, and 120 h at 37 °C and 5% CO_2. For tracer studies, preincubation medium was exchanged after 3 h for custom cystine/cysteine-free medium (Gibco) supplemented with $^{13}C_3$,^{15}N-cysteine (Sigma, final concentration 0.3 mM) and cells were treated with 1 and 10 μM sulfasalazine, 10 nM TCDD or vehicle (DMSO) for 48 h.

Cytotoxicity Measurement. Lactate dehydrogenase (LDH) release into the cell culture medium was measured by the cytotoxicity detection kit (Roche Applied Science, Indianapolis, IN). Medium was collected at 24, 48, and 120 h after treatment. Cells were washed with phosphate-buffered saline (PBS) and lysed with 1% Triton-X-100 in PBS for 4 h at 37 °C. LDH activity was determined in the medium and lysate by measuring absorbance at 490 nm. The LDH released into the medium was normalized to total LDH (in medium + in cell lysate).

https://doi.org/10.1021/acs.chemrestox.3c00017
Chem. Res. Toxicol. 2023, 36, 900−915

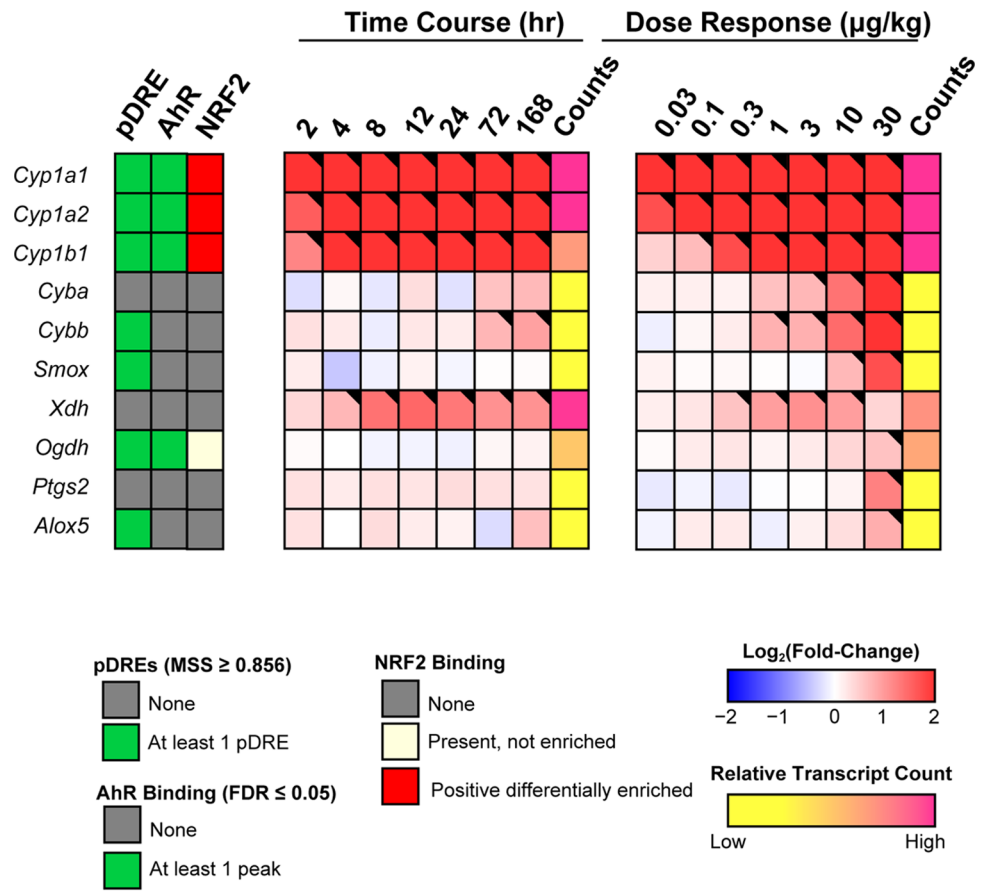

Figure 1. TCDD-induced genes associated with enzymatic activity and increased ROS levels. Hepatic gene expression was assessed in time course and dose response studies. In the time course study, male C57BL/6Ncrl mice (n = 3) were administered a single bolus dose of 30 μg/kg TCDD. Liver samples were collected at the corresponding timepoint, while in the dose response study male C57BL/6Ncrl mice (n = 3) were orally gavaged with sesame oil vehicle or TCDD every 4 days for 28 days. The presence of putative dioxin response elements (pDREs) and AhR genomic binding is indicated as a green box. Positive differentially enriched NRF2 is depicted by a red box. Color scale (blue to red) represents the $\log_2$(fold change) in gene expression determined by RNAseq analysis. Counts represent the maximum raw number of aligned reads to each transcript where lower levels of expression (≤500 reads) are depicted in yellow and higher expression (≥10,000) are depicted in pink. Differential expression with a posterior probability ($P1(t)$) > 0.80 is indicated by a black triangle in the top right corner of a heatmap tile. Abbreviations: arachidonate 5-lipoxygenase (*Alox5*), cytochrome b-245 α chain (*Cyba*), cytochrome b-245 β chain (*Cybb*), cytochrome P450 1A1 (*Cyp1a1*), 1A2 (*Cyp1a2*), 1B1 (*Cyp1b11*), 2-oxoglutarate dehydrogenase (*Ogdh*), prostaglandin-endoperoxide synthase 2 (*Ptgs2*), spermine oxidase (*Smox*), xanthine dehydrogenase (*Xdh*).

RESULTS

Gross Morphology, Histopathology, and Differential Gene Expression. This study focused on the dose-dependent effects of TCDD on the transsulfuration pathway in male mice since they exhibit greater sensitivity compared to females.[31,33,38,43] Absolute and relative liver weights increased 18−30 and 18−57% at 1−10 and 0.3−30 μg/kg TCDD, respectively, with no change in daily chow consumption.[38] In addition, absolute and relative gonadal white adipose tissue weights were reduced, with no change in terminal brown adipose tissue weights. Although a modest increase in serum alanine aminotransferase (ALT) levels was reported, no evidence of overt toxicity was reported.[23,38] Hepatic fat accumulation, inflammation, fibrosis, and bile duct proliferation were dose-dependently induced in male mice treated with TCDD every 4 days for 28 days.[21] Hepatocyte vacuolization (fatty change) and minimal/slight hepatocyte necrosis were first evident at 0.3 μg/kg TCDD. Leukocyte infiltration was present at ≥3 μg/kg, while F4/80 staining confirmed the leukocyte foci consisted primarily of macrophages. Bile duct proliferation with proximal inflammation (pericholangitis) was only reported at 30 μg/kg in male mice. The doses and treatment regimen resulted in hepatic TCDD levels that approached steady state and induced AhR target genes including those associated with increased ROS levels (Figure 1). Interestingly, several ROS producers including CYP1A1, 1A2, and 1B1 also exhibited NRF2 genomic enrichment in addition to AhR enrichment at 2 h following a single oral gavage of 30 μg/kg TCDD. In contrast, *Xdh*, a gene encoding the potent superoxide producer xanthine dehydrogenase, had no pDREs and exhibited no AhR or NRF2 genomic binding at 2 h. Therefore, histopathology, ALT levels, and gross morphology suggest the effects on gene expression, protein levels, and metabolite levels to be discussed below are not due to overt toxicity following oral gavage with TCDD every 4 days for 28 days.

Effects on the Transsulfuration Pathway. We have previously reported that TCDD dose-dependently dysregulated gene expression and metabolite levels associated with the methionine cycle in OCM.[26] Since these intermediates are shared with the transsulfuration pathway and can impose allosteric effects on OCM, we investigated the potential

https://doi.org/10.1021/acs.chemrestox.3c00017
Chem. Res. Toxicol. 2023, 36, 900−915

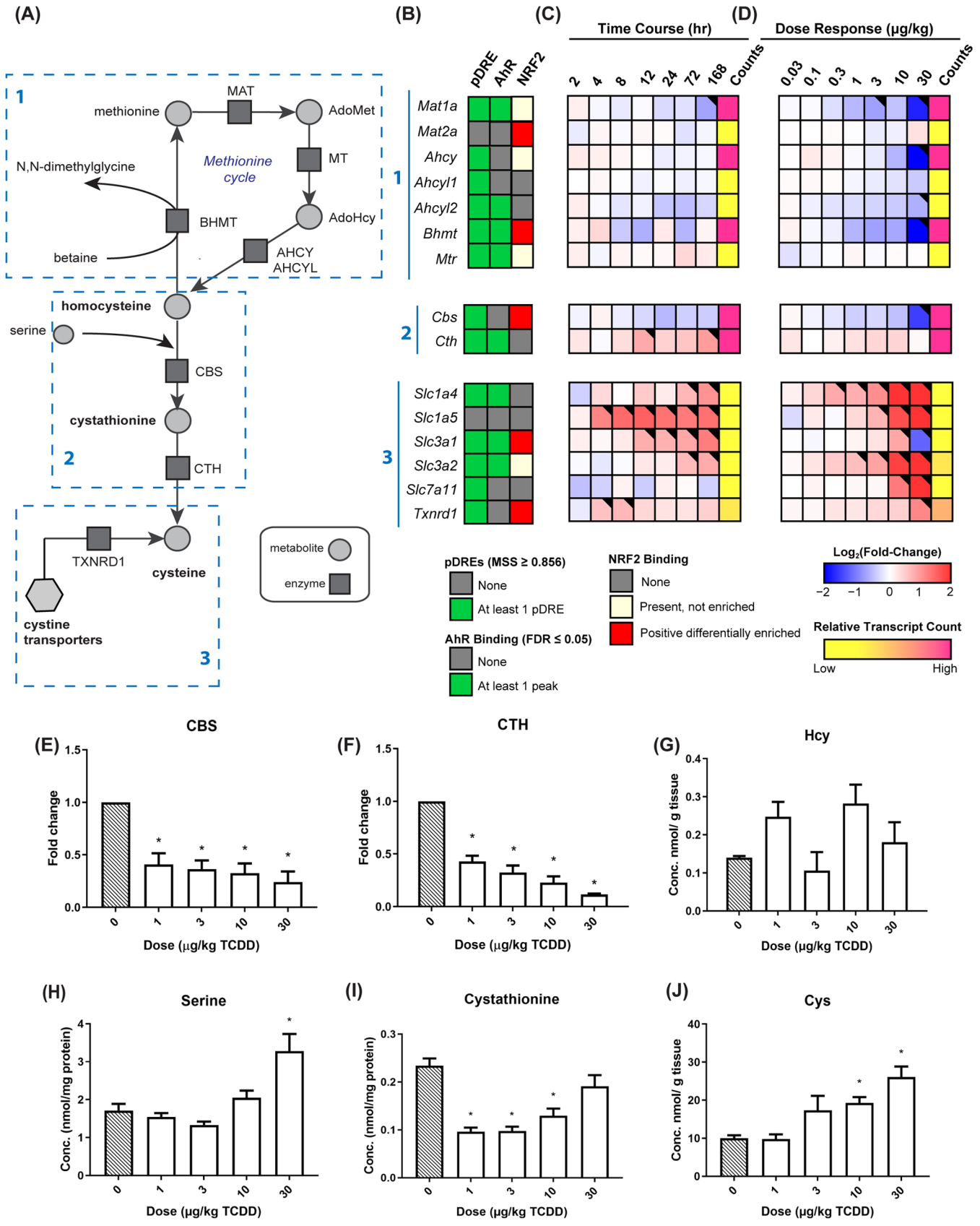

Figure 2. Effects of TCDD on the transsulfuration pathway. (A) Schematic depicting transsulfuration enzymes and metabolites. Numbers indicate genes presented in the (1) methionine cycle, (2) transsulfuration pathway, and (3) cystine transport and reduction. (B) Presence of putative dioxin response elements (pDREs) and AhR genomic binding to the intragenic region (10 kb upstream of the TSS to TES) is represented as a green box. Positive differentially enriched NRF2 is depicted by a red box. Numbers indicate genes associated with the (1) methionine cycle, (2) transsulfuration pathway, and (3) cystine transport and reduction. Hepatic gene expression associated with transsulfuration assessed by RNAseq in

https://doi.org/10.1021/acs.chemrestox.3c00017
Chem. Res. Toxicol. 2023, 36, 900−915

Figure 2. continued

a (C) time course following a single oral gavage of 30 μg/kg TCDD and (D) dose response study following oral gavage with TCDD every 4 days for 28 days. Color scale (blue to red) represents the $\log_2$(fold change) in gene expression determined by RNAseq analysis. Counts represent the maximum raw number of aligned reads of each transcript where a lower level of expression ($\leq$500 reads) is depicted in yellow and higher expression ($\geq$10,000) is depicted in pink. A black triangle in the top right corner of a heatmap tile denotes a change in gene expression (|fold-change| $\geq$1.5; $P1(t) \geq 0.80$). Hepatic (E) CBS and CTH protein levels were determined by Western blot in male mice orally gavaged with sesame oil vehicle or TCDD every 4 days for 28 days. Levels of (G) homocysteine, (H) serine, (I) cystathionine, and (J) cysteine in liver extracts from male C57BL/6Ncrl mice orally gavaged every 4 days for 28 days with sesame oil vehicle or TCDD measured by liquid chromatography−mass spectrometry (LC-MS) following NEM conjugation. Asterisk (*) denotes $p < 0.05$ determined by one-way analysis of variance (ANOVA) with a Dunnett's post hoc test. Error bars represent + standard error of the mean. Numbers 1, 2, and 3 indicate genes presented in the (1) methionine cycle, (2) transsulfuration pathway, and (3) cystine transport. Abbreviations: *S*-adenosylhomocysteine hydrolase (*Ahcy*), *S*-adenosylhomocysteine hydrolase-like isoform 1 or 2 (*Ahcyl1*, *Ahcyl2*), betaine-homocysteine methyltransferase (*Bhmt*), cystathionine β-synthase (*Cbs*), cystathionine γ-lyase (*Cth*), cysteine (Cys), homocysteine (Hcy), *S*-adenosylmethionine synthase isoform 1a, 2a, or 2b (*Mat1a*, *Mat2a*, *Mat2b*), methyltransferase (*Mt*), methionine synthase (*Mtr*), solute carrier family 1 member 4 and 5 (*Slc1a4*, *Slc1a5*), cystine/glutamate antiporter Xc^- system light chain (*Slc7a11*) and heavy chain (*Slc3a2*), transcription end site (TES), transcription start site (TSS), thioredoxin reductase 1 (*Txnrd1*).

consequences of TCDD treatment on cysteine levels by integrating complementary ChIPseq, RNAseq, and metabolomics datasets (Figure 2). Dose response studies showed that, in addition to repression of the methionine cycle/OCM, cystathionine β-synthase (*Cbs*) mRNA levels were dose-dependently reduced 2.9-fold (Figure 2D). Moreover, CBS and cystathionine γ-lyase (CTH) protein levels were reduced at doses as low as 1.0 μg/kg (Figure 2E,F). Both *Cbs* and *Cth* possessed pDREs, but only *Cth* exhibited AhR enrichment at 2 h following a single oral gavage of 30 μg/kg TCDD suggesting the dose-dependent repression of *Cbs* may not involve direct AhR regulation. Furthermore, *Bhmt* repression, reduced cobalamin levels required for methionine synthase (MTR) activity, and the repression of CBS mRNA and protein levels are consistent with the increased levels of homocysteic acid, the spontaneous oxidation product of homocysteine.[26,44] Although homocysteine (Hcy) levels were unchanged, the levels of serine, which undergoes condensation with homocysteine to produce cystathionine, were increased, whereas cystathionine levels decreased at 1, 3, and 10 μg/kg TCDD (Figure 2G,I). The recovery of cystathionine levels at 30 μg/kg TCDD has been partially attributed to *Mat2a* induction and increased production of *S*-adenosylmethionine (SAM), which is a potent allosteric CBS activator.[26,45] Therefore, homocysteine does not enter the transsulfuration pathway nor is it used as a substrate for re-methylation to methionine catalyzed by betaine-homocysteine *S*-methyltransferase (BHMT) or MTR, but instead undergoes oxidation as indicated by the dose-dependent increase in homocysteic acid levels.[26]

Next, we examined the consequences of CBS and CTH repression and the unexpected increase in the levels of cysteine, the limiting amino acid in GSH synthesis (Figure 2J). In response to the repression of the methionine cycle and the transsulfuration pathway, intracellular cysteine was likely imported by the dose-dependent induction of cysteine transporters such as the cystine/glutamate antiporter Xc^- system to support GSH synthesis.[46] Specifically, *Slc1a4*, *1a5*, and *7a11* were induced 8.1-, 7.3-, and 79.3-fold at 30 μg/kg TCDD as assessed by RNAseq and confirmed by quantitative reverse transcription polymerase chain reaction (qRT-PCR) (Figures 2B−D and S3). Moreover, cystine/glutamate Xc^- antiporter protein level was also increased following TCDD treatment (Figure S4). The cystine/glutamate antiporter Xc^- system consists of the xCT light chain (*Slc7a11*), which confers specificity for cystine transport when linked by a disulfide bridge to the 4F2 heavy chain (*Slc3a2* induced 4.3-fold) and imports one cystine into the cell for each glutamate exported. The lack of AhR or NRF2 genomic enrichment is likely due to the short 2 h exposure duration with 30 μg/kg TCDD since *Slc7a11* induction by electrophilic agents is known to be mediated by NRF2.[47] Once inside the cell, cystine is reduced by TXNRD1 (*Txnrd1* induced 3.3-fold) to two cysteine molecules.[46,48]

In addition to their canonical cysteine synthesis reactions, CBS and CTH metabolize homocysteine and/or cysteine to produce hydrogen sulfide (H_2S), an endogenous signaling gas that exerts diverse physiological effects (Figure 3A). Consistent with the repression of CBS and CTH by TCDD, H_2S levels also exhibited a dose-dependent decrease (Figure 3F). Lower H_2S levels may also be due to the 4.5-fold repression of mercaptopyruvate sulfurtransferase (*Mpst*), which catalyzes the desulfuration of 3-mercaptopyruvate to produce pyruvate and a persulfide product that releases H_2S. Moreover, genes associated with the sulfide oxidation pathway that oxidize H_2S to thiosulfate and sulfate were dose-dependently repressed. Specifically, ETHE1 persulfide dioxygenase (*Ethe1*), thiosulfate sulfurtransferase (*Tst*), and sulfite oxidase (*Suox*) were repressed 5.9-, 2.5-, and 4.5-fold at 30 μg/kg TCDD, respectively, suggesting that reduced H_2S levels could not be ascribed to increased oxidation. *Sqrdl*, *Ethe1*, *Tst*, and *Suox* exhibited mixed AhR and NRF2 genomic enrichment 2 h after oral gavage with 30 μg/kg TCDD (Figure 3C−E). Together, the data suggest that reductions in H_2S levels are due to reduced expression of CBS, CTH, and MPST as opposed to increased metabolism in the sulfide oxidation pathway.

Effects on Glutathione and Ophthalmic Acid Synthesis. Repression of the transsulfuration pathway with the induction of cysteine transporters prompted us to assess the dose-dependent effects of TCDD on GSH biosynthesis as well as GSSG recycling and efflux (Figure 4). Although GSH and GSSG levels in hepatic extracts did not significantly change following oral gavage every 4 days for 28 days, the GSH:GSSG ratio decreased from 80 to 4 at 30 μg/kg TCDD, as expected due to the induction of oxidative stress (Figure 4E−G). Increased levels of cysteine (Figure 2J), glutamate, and glycine have also been reported for other inducers of oxidative stress such as acetaminophen (Figure 4I,J).[49] In addition, glutamate-cysteine ligase catalytic subunit (*Gclc*), glutathione synthetase (*Gss*), glutathione peroxidase 2 (*Gpx2*), glutathione peroxidase 3 (*Gpx3*), and glutathione disulfide reductase (*Gsr*) were induced 1.7-, 2.4-, 40.3-, 6.7-, and 3.8-fold, respectively (Figure 4D). Increased expression of *Gpx2* following TCDD administration was confirmed at the protein level (Figure

https://doi.org/10.1021/acs.chemrestox.3c00017
Chem. Res. Toxicol. 2023, 36, 900−915

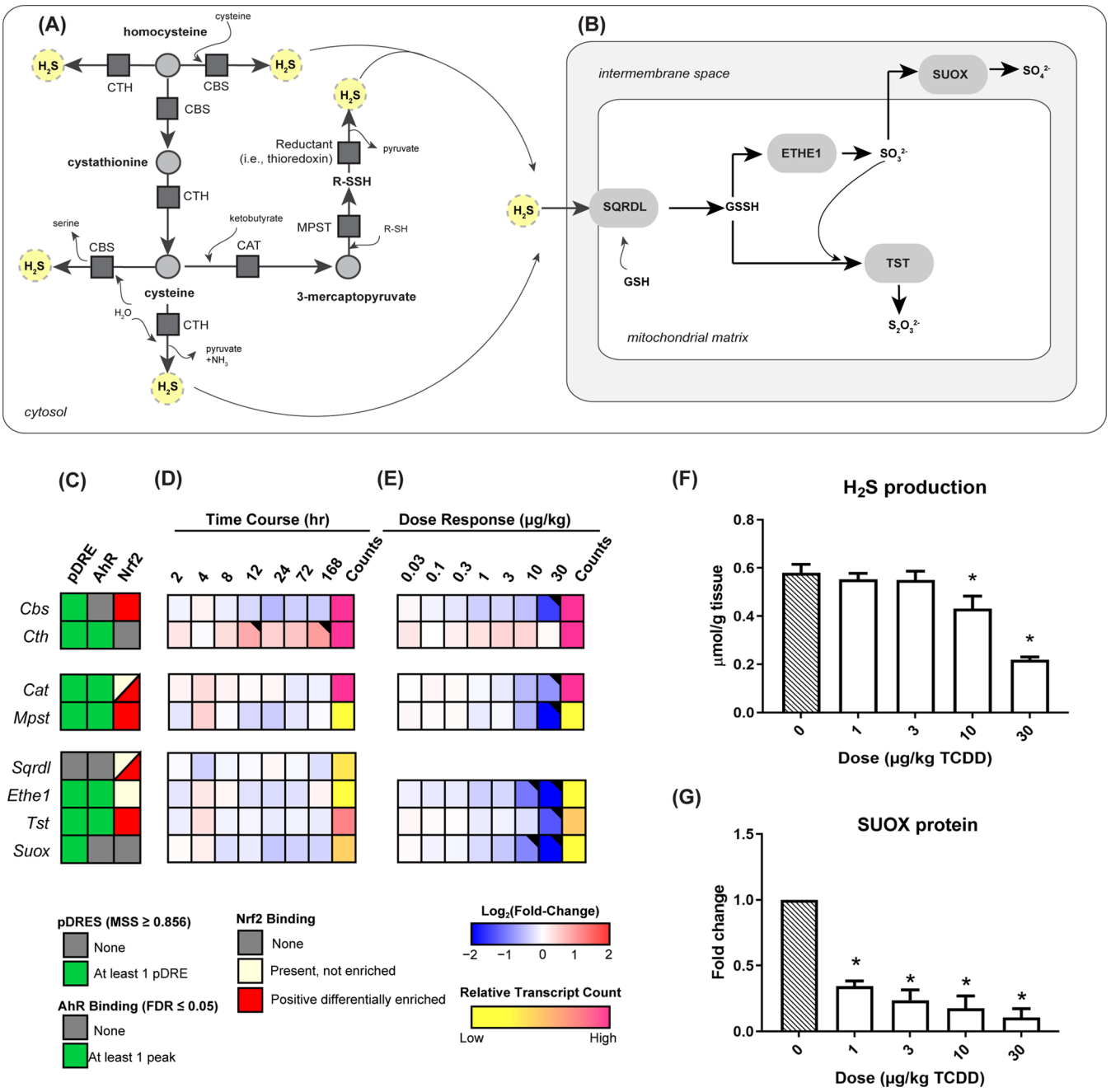

Figure 3. Effects of TCDD on H_2S production and the sulfide oxidation pathway. (A) Schematic depicting H_2S-producing reactions. (B) Schematic depicting sulfide oxidation pathway. (C) Presence of putative dioxin response elements (pDREs) and AhR genomic binding to the intragenic region (10 kb upstream of the TSS to TES) represented as a green box. Positive differentially enriched NRF2 is depicted by a red box. Hepatic differential gene expression associated with the transsulfuration pathway assessed by RNAseq in a (D) time course following a single oral gavage of 30 μg/kg TCDD and (E) dose response study following oral gavage with TCDD every 4 days for 28 days. Color scale (blue to red) represents the $\log_2$(fold change) in gene expression. Counts represent the maximum raw number of aligned reads of each transcript where a lower level of expression (≤500 reads) is depicted in yellow and higher expression (≥10,000) is depicted in pink. A black triangle in the top right corner of a heatmap tile denotes a change in gene expression (|fold-change| ≥ 1.5; $P1(t) \geq 0.80$). (F) Hepatic H_2S levels were assessed using OxiSelect Free Hydrogen Sulfide Gas Assay (Cell Biolabs). (G) Hepatic Soux protein levels were determined by Western blot in male C57BL/6Ncrl mice orally gavaged with sesame oil vehicle or TCDD every 4 days for 28 days. Asterisk (*) denotes $p < 0.05$ determined by one-way ANOVA with a Dunnett's post hoc test. Error bars represent + standard error of the mean. Abbreviations: cysteine aminotransferase (*Cat*), cystathionine β-synthase (*Cbs*), cystathionine γ-lyase (*Cth*), persulfide dioxygenase (*Ethe1*), 3-mercaptopyruvate sulfurtransferase (*Mpst*), sulfur acceptor (R-SH); persulfide (R-SSH); sulfite oxidase (*Suox*), quinone oxidoreductase (*Sqrdl*); transcription end site (TES), transcription start site (TSS), thiosulfate sulfurtransferase (*Tst*).

2H). Genes associated with GSH synthesis, recycling, and GSSG efflux exhibited AhR and/or NRF2 genomic enrichment 2 h after a single dose of 30 μg/kg TCDD in the presence of a pDRE. Although *Gsr* is induced 3.8-fold at 30 μg/kg TCDD, accumulating GSSG can be actively transported out of the cell to maintain intracellular redox when ROS levels overcome the

https://doi.org/10.1021/acs.chemrestox.3c00017
Chem. Res. Toxicol. 2023, 36, 900−915

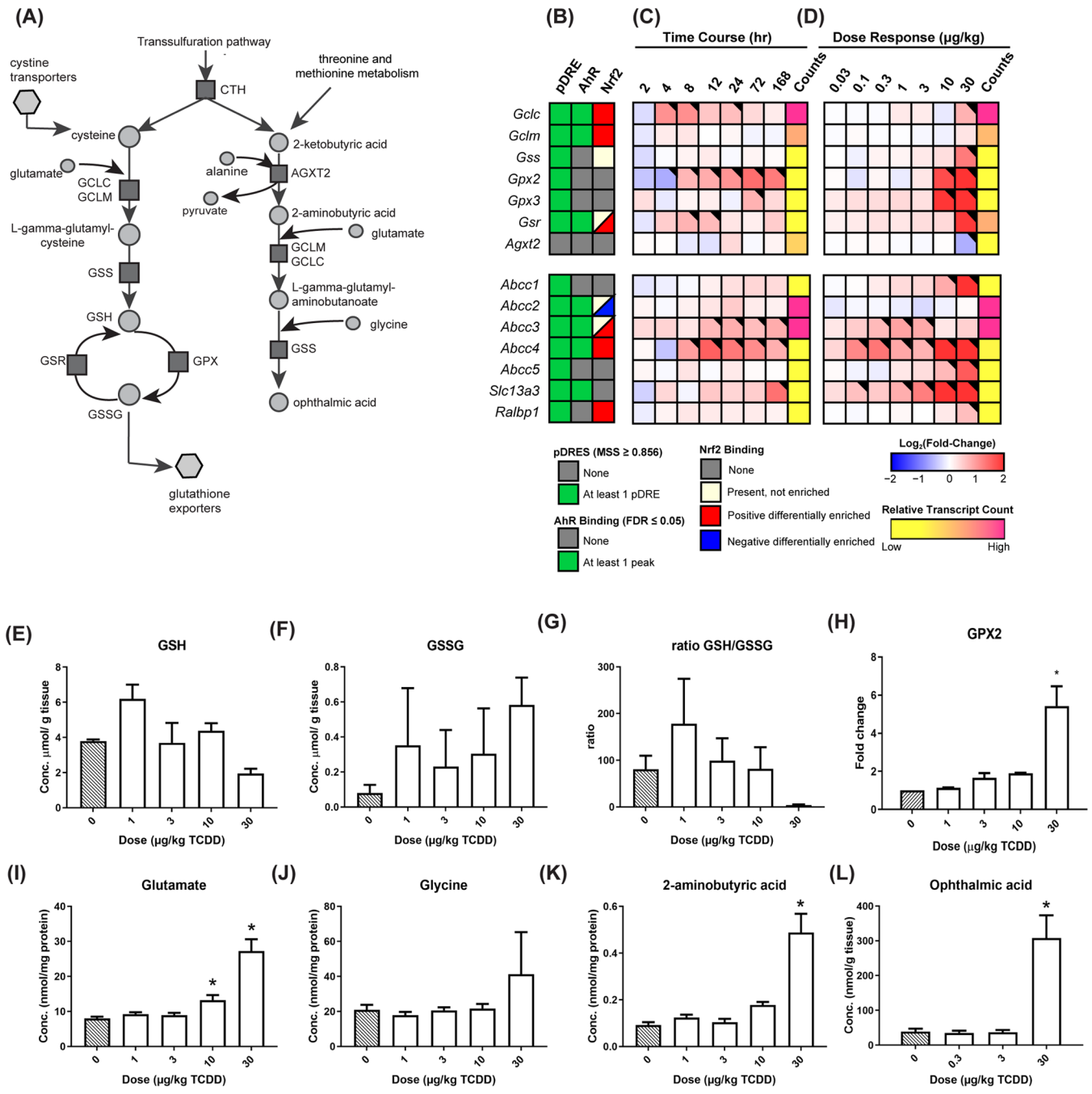

Figure 4. TCDD-elicited effects on glutathione (GSH) and ophthalmic acid synthesis. (A) Schematic depicting enzymes and metabolites associated with glutathione and ophthalmic acid synthesis. (B) Presence of putative dioxin response elements (pDREs) and AhR genomic binding to the intragenic region (10 kb upstream of the TSS to TES) is represented as a green box. Green (unchanged)/red (increased)/blue(decreased) boxes indicate more than one site of genomic AhR enrichment (and effect of TCDD). Hepatic gene expression associated with glutathione and ophthalmic acid synthesis was assessed by RNAseq in a (C) time-course and (D) dose-dependent manner. The blue/red color scale represents the $\log_2$(fold change) in gene expression. Counts represent the maximum raw number of aligned reads to each transcript where a lower level of expression (≤500 reads) is depicted in yellow with higher expression (≥10,000) depicted in pink. A black triangle in the top right corner of a heatmap tile denotes a change in gene expression (lfold-changel ≥ 1.5; $P1(t) \geq 0.80$). Hepatic (E) reduced glutathione (GSH), (F) oxidized glutathione (GSSG), (G) GSH:GSSG ratio, (I) glutamate, (J) glycine, (K) 2-aminobutyric acid, and (L) ophthalmic acid were measured by LC-MS in male C57BL/6Ncrl mice orally gavaged every 4 days for 28 days with sesame oil vehicle or TCDD (0.3 or 1−30 μg/kg). Hepatic (H) GPX2 protein level was determined by Western blot in liver extracts prepared from male C57BL/6Ncrl mice orally gavaged every 4 days for 28 days with sesame oil vehicle or 1−30 μg/kg TCDD. Asterisk (*) denotes $p < 0.05$ determined by one-way ANOVA with Dunnett's post hoc test. Error bars represent + standard error of the mean. Abbreviations: ATP binding cassette subfamily C member 1, 2, 3, 4, 5 (*Abcc2*, *Abcc3*, *Abcc4*, *Abcc5*), alanine-glyoxylate aminotransferase isoform 2 (*Agxt2*), cysteine aminotransferase (*Cat*), glutamate-cysteine ligase, catalytic subunit (*Gclc*), glutamate-cysteine ligase regulatory subunit (*Gclm*), glutathione peroxidase 2, 3 (*Gpx2*, *Gpx3*), reduced glutathione (GSH), glutathione disulfide reductase (*Gsr*), glutathione synthetase (*Gss*); oxidized glutathione (GSSG), 3-mercaptopyruvate sulfurtransferase (*Mpst*), RalA binding protein 1 (*Ralbp1*), solute carrier family 13 member 3 (*Slc13a3*); transcription end site (TES), transcription start site (TSS).

https://doi.org/10.1021/acs.chemrestox.3c00017
Chem. Res. Toxicol. 2023, 36, 900−915

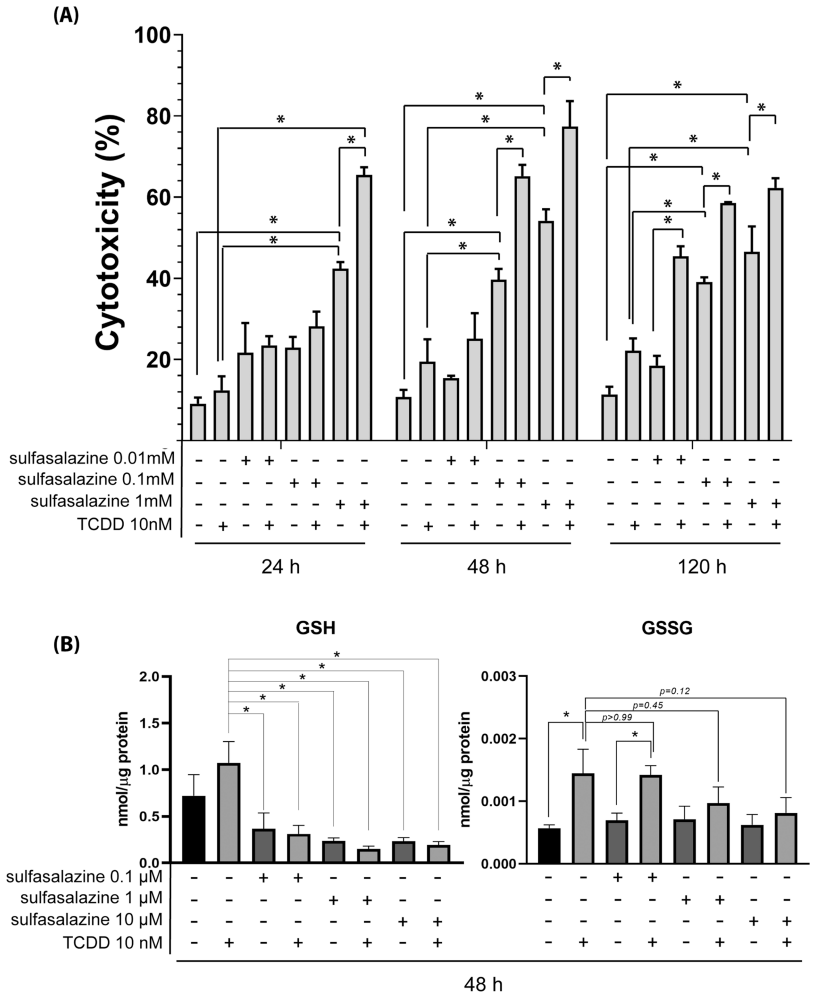

Figure 5. Effect of TCDD on glutathione (GSH) and oxidized glutathione (GSSG) levels and cytotoxicity in primary mouse hepatocytes in the absence and presence of the cystine/glutamate antiporter Xc^- system inhibitor, sulfasalazine. (A) Primary mouse hepatocytes isolated from wild-type male C57BL/6Ncrl mice were treated 3 h after plating (n = 3 wells) with TCDD and/or sulfasalazine as indicated. Cytotoxicity was measured by measuring LDH release in media. Asterisk (*) indicates $p \leq 0.05$ between compared groups. (B) Primary mouse hepatocytes isolated from wild-type male C57BL/6Ncrl mice were treated 3 h after plating (n = 4) with TCDD and/or sulfasalazine as indicated. GSH and GSSG levels were measured 48 h after treatment by LC-MS. Error bars represent + standard error of the mean. Asterisk (*) denotes $p < 0.05$ determined by two-way ANOVA with a Tukey's post hoc test. Abbreviations: reduced glutathione (GSH), oxidized glutathione (GSSG), 2,3,7,8-tetrachlorodibenzo-*p*-dioxin (TCDD), lactate dehydrogenase (LDH).

capacity to reduce GSSH to GSH. GSH and GSSG efflux transporters, *Abcc1*, *2*, *3*, *4*, and *5* as well as *Slc13a3* and *Ralbp1* exhibited time- and dose-dependent induction with AhR and/or NRF2 genomic enrichment (Figure 4B–D).[50−52]

In addition to cysteine, the metabolism of cystathionine by CTH also produces 2-ketobutyric acid, which can be transaminated to 2-aminobutyric acid, an intermediate structurally identical to cysteine except for the substitution of the sulfhydryl moiety with a methyl group.[53] 2-Ketobutyric acid, also produced from threonine and methionine metabolism,[54,55] can undergo condensation with glutamate catalyzed by GCL to produce L-γ-glutamyl-aminobutanoate, which is then ligated to glycine by GSS to yield ophthalmic acid, a biomarker of oxidative stress indicating GSH consumption.[49] 2-Aminobutyric acid and ophthalmic acid levels were induced 5.3- and 7.9-fold, respectively, at 30 μg/kg TCDD coinciding with the recovery of cystathionine levels at 30 μg/kg TCDD attributed to *Mat2a* induction.[26]

The effects of TCDD on GSH metabolism and cytotoxicity were further examined in primary mouse hepatocytes (Figure 5). As reported *in vivo*, 10 nM TCDD, a dose that induced *Cyp1a1* 743-fold, did not affect GSH levels but increased GSSG levels 2-fold at 24 and 48 h (Figure 5B) decreasing the in vitro GSH/GSSG ratio from 904 to 328 and from 347 to 280 after 24 and 48 h of treatment, respectively. Unlike in vivo where expression was negligible in control samples, the cystine/glutamate antiporter Xc^- system was expressed in primary hepatocyte under conventional culture conditions as previously reported (Figure S2).[56] This enabled an investigation of the role of the cystine/glutamate antiporter Xc^- system in TCDD-elicited cytotoxicity. Figure 5A shows that in the absence of TCDD, sulfasalazine, a cystine/glutamate antiporter Xc^- system inhibitor, exhibited dose-dependent cytotoxicity alone.[57] However, cytotoxicity as measured by lactate dehydrogenase activity in media was greater when hepatocytes were cotreated with sulfasalazine and 10 nM TCDD. Furthermore, sulfasalazine cotreatment with TCDD elicited a further decrease in GSH while GSSG levels also trended downward (not significant) compared to TCDD alone (Figure 5B).

https://doi.org/10.1021/acs.chemrestox.3c00017
Chem. Res. Toxicol. 2023, 36, 900−915

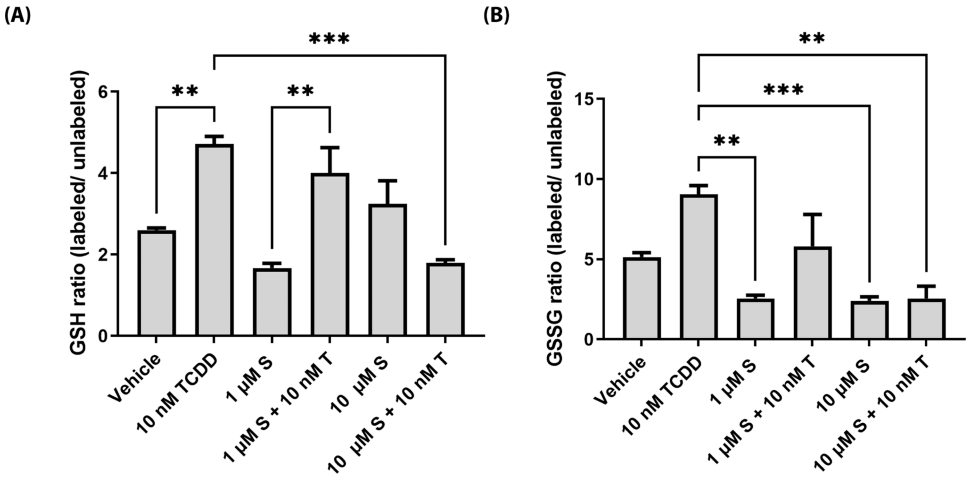

Figure 6. Tracer studies examining the effect of TCDD on (A) glutathione (GSH) and (B) oxidized glutathione (GSSG) levels in primary mouse hepatocytes cultured in medium with $^{13}C_3$,^{15}N-cysteine in the absence and presence of the cystine/glutamate antiporter Xc^- system inhibitor, sulfasalazine. Primary mouse hepatocytes isolated from wild-type male C57BL/6Ncrl mice were culture in $^{13}C_3$,^{15}N-cysteine-containing medium and treated 3 h after plating (n = 4) with TCDD and/or sulfasalazine as indicated. GSH and GSSG levels were measured 48 h after treatment by LC-MS. Error bars represent ± standard error of the mean. Asterisk denoting $^{**}p < 0.01$, or $^{***}p < 0.001$ were determined by two-way ANOVA with Tukey's post hoc test. Abbreviations: reduced glutathione (GSH), oxidized glutathione (GSSG), sulfasalazine (S), 2,3,7,8-tetrachlorodibenzo-*p*-dioxin (T).

To further examine the role of the cystine/glutamate antiporter Xc^- system in TCDD cytotoxicity, $^{13}C_3$,$^{15}N_1$-GSH as well as $^{13}C_3$,$^{15}N_1$- and $^{13}C_6$,$^{15}N_2$-GSSG levels were measured at 48 h after treatment with 10 nM TCDD and/or sulfasalazine in primary hepatocytes cultured in media containing $^{13}C_3$,^{15}N-cysteine (Figure 6). $^{13}C_3$,$^{15}N_1$-GSH as well as $^{13}C_3$,$^{15}N_1$- and $^{13}C_6$,$^{15}N_2$-GSSG levels increased in response to 10 nM TCDD. Sulfasalazine at 10 μM, but not at 1 μM, decreased the levels of $^{13}C_3$,$^{15}N_1$-GSH as well as $^{13}C_3$,$^{15}N_1$- and $^{13}C_6$,$^{15}N_2$-GSSG compared to TCDD treatment alone suggesting that 1 μM sulfasalazine was too low to overcome the induction of the cystine/glutamate antiporter Xc^- system in response to TCDD. These results indicate that in response to TCDD-elicited oxidative stress, cystine import is increased via the cystine/glutamate antiporter Xc^- system to support GSH biosynthesis due to inhibition of the transsulfuration pathway and the increased oxidation of GSH to GSSG.

Effects on Protein *S*-Glutathionylation. GSH can also reversibly oxidize cysteinyl residues in proteins via S-glutathionylation to introduce the three amino acid moiety and a net negative charge that may alter the secondary structure, location, and function of various regulatory, structural, and metabolic proteins. Moreover, protein S-glutathionylation provides protection from irreversible oxidation.[5] A representative western blot shows changes in the pattern and levels of global protein S-glutathionylation in hepatic extracts prepared from mice treated with TCDD every 4 days for 28 days (Figure 7A,B) with protein S-glutathionylation levels greatest for 40−55 kDa proteins (Figure 7C).

In addition to spontaneous protein S-glutathionylation under oxidative conditions, oxidized cysteinyl residues on proteins can also undergo rapid conjugation with GSH catalyzed by glutathione *S*-transferase p1 and p2 (GSTP1 and 2).[58−60] *Gstp1* and *p2* were both induced within 4 h of oral gavage with 30 μg/kg TCDD (Figure 7E). Although the more highly expressed *Gstp1* was repressed in the 28 days dose response study, *Gstp2* exhibited dose-dependent induction with a 3.6-fold increase at 30 μg/kg TCDD (Figure 7F). Moreover, glutaredoxin (GLRX) and GLRX2 possess both protein S-glutathionylation and de-glutathionylation activities depending on the GSH/GSSG ratio.[61] *Glrx* and *Glrx2* were dose-dependently repressed 1.5- and 2.9-fold, respectively. Thioredoxin1 and 2 (TXN1 and 2) as well as protein disulfide isomerases 3, 4, 5, and 5 (PDIA3, 4, 5, and 6) also possess de-glutathionylation activity but are less efficient than GLRX.[62] TCDD elicited negligible effects on *Txn1* and *2*, while *Pdia3*, *4*, *5*, and *6* were repressed 1.6-, 2.4-, 4.2-, and 2.0-fold, respectively. Lastly, sulfiredoxin (SRXN1) catalyzes the de-glutathionylation of distinct proteins in response to oxidative and/or nitrosative stress and exhibited a 16.9-fold dose-dependent induction following treatment with 30 μg/kg TCDD.[63] Reducing equivalents required for de-glutathionylation reactions are provided by NADPH catalyzed by glutathione reductase (GSR), or thioredoxin reductases (TXNRD1, 2, and 3).[64,65] The more highly expressed reductases, *Gsr* and *Txnrd1*, were induced in the time course and dose response studies, while *Txnrd2* and *3* were repressed at the highest dose. It is notable that not all of the genes listed in Figure 7D showed NRF2 genomic enrichment 2 h after oral gavage with 30 μg/kg TCDD while others had multiple sites of NRF2 enrichment with constitutive peaks exhibiting increased genomic binding (i.e., positive differential enrichment as determined by ChiP PCR) following TCDD treatment. In contrast, only *Gsr*, *Txn2*, *Txnrd2*, and *Srxn1* exhibited AhR genomic enrichment and in each case, in the presence of a pDRE. Previous studies have suggested cooperation between AhR and NRF2 in the regulation of gene expression.[39,66] Overall, the data are consistent with an increase in protein S-glutathionylation in response to TCDD-induced oxidative stress.

DISCUSSION

TCDD dose-dependently induces the expression of thousands of genes in the liver, many of which encode for enzymes that produce ROS as a reaction byproduct. Under normal

https://doi.org/10.1021/acs.chemrestox.3c00017
Chem. Res. Toxicol. 2023, 36, 900−915

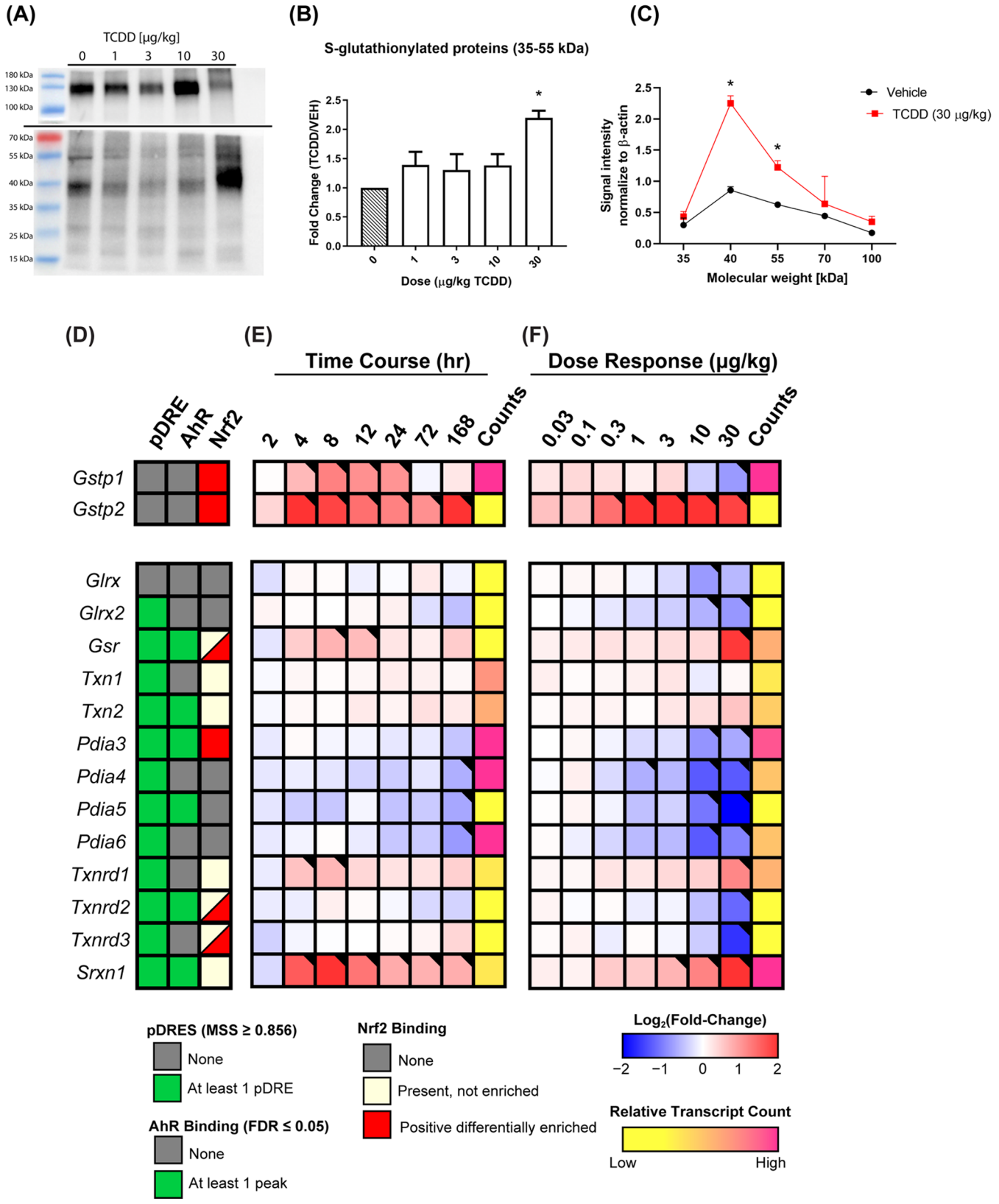

Figure 7. Effect of TCDD on protein S-glutathionylation in hepatic extracts and expression of genes associated with glutathionylation and deglutathionylation. Male C57BL/6Ncrl mice (n = 3) were orally gavaged with sesame oil vehicle or 1−30 μg/kg TCDD every 4 days for 28 days. (A) Representative immunoblot for global protein S-glutathionylation levels in hepatic extracts. Proteins were analyzed by SDS-PAGE (10% gel) using nonreducing conditions, transferred to poly(vinylidene difluoride) (PVDF) membrane, and probed with anti-protein S-glutathionylation antibody. Brightness, contrast, and color balance were adjusted to optimize visualization. (B) Densitometric analysis of S-glutathionylated protein levels (35−55 kDa). Asterisk (*) denotes $p < 0.05$ determined by one-way ANOVA with Dunnett's post hoc test. Error bars represent + standard error of the mean. (C) Comparison of signal intensity of individual protein bands. Asterisk (*) denotes $p < 0.05$ determined by two-way ANOVA

https://doi.org/10.1021/acs.chemrestox.3c00017
Chem. Res. Toxicol. 2023, 36, 900−915

Figure 7. continued

with Sidak's post hoc test. (D) The presence of putative dioxin response elements (pDREs) and AhR binding to the intragenic region (10 kb upstream of the TSS to TES) is represented as a green box. Positive differentially enriched Nrf2 is depicted by a red box. Green (unchanged)/red (increased) boxes indicate more than one site of genomic AhR enrichment (and the effect of TCDD). Hepatic expression of genes associated with glutathione and ophthalmic acid synthesis was assessed by RNAseq in a (E) time-course and (F) dose-dependent manner. Color scale represents the $\log_2$(fold change) in gene expression. Counts represent the maximum raw number of aligned reads to each transcript where a lower level of expression (≤500 reads) is depicted in yellow with higher expression (≥10,000) depicted in pink. A black triangle in the top right corner of a heatmap tile denotes significant differential gene expression (lfold-changel ≥ 1.5; $P1(t) \geq 0.80$). Abbreviations: glutaredoxin (Glrx), glutathione reductase (Gsr), glutathione *S*-transferase Pi (Gstp), protein disulfide isomerase associated (Pdia), sulfiredoxin (Srxn), 2,3,7,8-tetrachlorodibenzo-*p*-dioxin (TCDD), transcription end site (TES), transcription start site (TSS), thioredoxin (Txn), thioredoxin reductase (Txnrd).

conditions, antioxidant systems protect critical cellular components while corrective measures rid cells of the stimulus responsible for excessive ROS levels in order to reestablish homeostasis. However, TCDD is not readily metabolized or excreted and induces persistent oxidative stress that can drain redox buffering requiring metabolic reprogramming to support antioxidant responses. For example, pyruvate kinase muscle isoform 2 (PKM2) induction redirects accumulating glycolytic intermediates to the pentose phosphate pathway and serine/glycine biosynthesis to support GSH biosynthesis and GSSG recycling in response to TCDD-induced ROS levels.[31] In addition to producing glycine and NADPH that may support GSH biosynthesis, serine/glycine biosynthesis is coupled to OCM via the folate and methionine cycles to generate *S*-adenosylmethionine (SAM), the methyl donating intermediate used for cellular biosynthesis and post-translational modifications. In turn, homocysteine, an intermediate in the methionine cycle, can feed into the transsulfuration pathway while SAM, a known regulator of CBS, links OCM and the transsulfuration pathway.[45,67] In this study, the consequences of methionine cycle and OCM reprogramming by TCDD were extended to further investigate effects on the transsulfuration pathway, which provides cysteine, the limiting amino acid required for GSH biosynthesis.[26]

Homocysteine can be converted to (i) methionine by 5-methyltetrahydrofolate-homocysteine methyltransferase (MTR) and betaine-homocysteine *S*-methyltransferase (BHMT) in the methionine cycle, or (ii) cystathionine and then cysteine by CBS and CTH in the transsulfuration pathway.[11] We have previously shown that TCDD repressed BHMT and CBS mRNA and protein levels.[26] Consequently, serine did not undergo condensation with homocysteine by CBS in the transsulfuration pathway resulting in reduced cystathionine levels. In addition, TCDD decreases cobalamin (Cbl) levels which compromise Cbl-dependent MTR activity.[68] Therefore, homocysteine is not re-methylated to methionine in the methionine cycle, but is oxidized as reflected in the increased levels of homocysteic acid, the spontaneous oxidation product of homocysteine, due to the oxidative conditions induced by TCDD.[26] The partial recovery of cystathionine at 30 μg/kg TCDD is in agreement with the induction of *S*-adenosylmethionine synthase isoform 2a (MAT2A). Increased SAM levels produced following MAT2a induction would allosterically activate CBS while further inhibiting MTR activity.[45] Moreover, TCDD dose-dependently reduced CTH protein levels, and to a lesser extent mRNA levels. In addition to homocysteine use as an intermediate in the transsulfuration pathway to produce cysteine, CBS and CTH also metabolize cysteine and homocysteine to produce H_2S, a key signaling molecule that regulates cell bioenergetics by reprogramming metabolism.[69] TCDD dose-dependently reduced H_2S levels consistent with the repression of CBS, CTH, and mercaptopyruvate sulfurtransferase (MPSF), the three main H_2S-generating enzymes. Genes in the sulfide oxidation pathway that are responsible for oxidative catabolism of H_2S were repressed suggesting reduced H_2S levels were not due to increased metabolism to sulfate and thiosulfate ions. Collectively, these results indicate TCDD repressed the transsulfuration pathway.

H_2S plays an important role in liver physiology as well as pathophysiology with disrupted levels associated with NAFLD and cirrhosis.[70] Moreover, exogenous H_2S treatment attenuated carbon tetrachloride-induced hepatotoxicity, liver cirrhosis, and portal hypertension.[71] Hepatic H_2S levels are reported to be lower in the high-fat-diet (HFD)-fed mice while exogenous H_2S treatment improved lipid metabolism and antioxidant potential in the fatty liver of HFD-induced obesity in mice.[72] Specifically, H_2S decreased lipid accumulation including triglyceride and total cholesterol, as well as repressed fatty acid synthase while inducing antioxidant enzyme activities.[73] Reduced H_2S levels are largely unexplored in TCDD-elicited hepatotoxicity and the progression of steatosis to steatohepatitis with fibrosis.

Cysteine levels, which are tightly regulated to maintain redox balance and minimize other adverse effects, were increased following treatment with TCDD, despite repression of the transsulfuration pathway. We attribute this to the ROS induction of the light chain subunit of the cystine/glutamate Xc^- antiporter that confers specificity for cystine transport.[46] Despite the higher levels of cysteine, the limiting amino acid required for GSH biosynthesis, as well as the increased glutamate and glycine levels, did not translate into substantive increases in hepatic GSH and GSSG levels. This may be partially explained by the induction of ABCC transporters that reestablish redox homeostasis.[74,75] However, TCDD did increase the levels of ophthalmic acid, a GSH analogue with no thiol group. Ophthalmic acid is synthesized by the GSH biosynthesis pathway but uses 2-aminobutyric acid as a substrate instead of cysteine, but is not metabolized further.[49] Ophthalmic acid accumulation correlates with GSH consumption and has been proposed as a biomarker for GSH depletion.[49] Furthermore, ophthalmic acid is reported to exert protective effects from oxidative stress by increasing the efflux of conjugated metabolites, inhibiting GSH efflux from hepatocytes, activating serine/glycine biosynthesis, and stimulating AMPK activity to increase GSH levels.[53] In contrast to these in vivo hepatic effects, TCDD did increase GSSG levels in primary mouse hepatocytes. Moreover, cotreatment with sulfasalazine, a cystine/glutamate Xc^- antiporter inhibitor,[57] increased the sensitivity of primary mouse hepatocytes to TCDD cytotoxicity. Together, these results support the conclusion that in response to TCDD-induced oxidative stress,

https://doi.org/10.1021/acs.chemrestox.3c00017
Chem. Res. Toxicol. 2023, 36, 900−915

hepatocytes increased GSH biosynthesis by inducing the cystine/glutamate Xc^- antiporter, which provides an alternative source of cysteine following the repression of the transsulfuration pathway. However, this is not reflected in increased GSH levels due to GSH utilization to maintain redox balance.

In addition to free radical scavenging, GSH can be conjugated to target proteins via cysteine sulfhydryl or sulfenic acid moieties. GSH conjugation protects proteins from the sequential oxidation of thiol groups to sulfonic acid that leads to proteosomal degradation. In addition, S-glutathionylation can alter the conformation of the protein target to affect function, interactions with other proteins, and cellular localization. The reversibility of S-glutathionylation can occur spontaneously in the presence of recovering GSH levels or be catalyzed by de-glutathionylation enzymes, to provide dynamic regulation.[5] More specifically, protein S-glutathionylation has been proposed as a mechanism to fine-tune cellular energy metabolism in response to varying oxidative stress levels with several glycolytic and TCA enzymes identified as S-glutathionylation targets that affect glucose flux.[60,76] TCDD increased the global levels of protein S-glutathionylation, especially in the 40−55 kDa range. Under the oxidative conditions, protein S-glutathionylation would also retain GSH in the cell, as well as protect proteins from further oxidation. GSTP1 and GSTP2, both of which possess protein S-glutathionylation activity, may also contribute to the increased global protein S-glutathionylation levels. De-glutathionylation, which is largely attributed to GLRX, was repressed by TCDD. Srxn1 was induced and serves a similar function, but has unknown in vivo de-glutathionylation significance.[77,78] Overall, the increase in global protein S-glutathionylation indicates increased GSH biosynthesis.

Although it is difficult to separate the direct effects of TCDD from secondary effects triggered by early disruptions, all effects observed in this work should be considered as TCDD-initiated. Moreover, neither overtoxicity nor effects that have been previously described as chronic, nonspecific, and have been linked to severe intoxication such as neural system damage and neuropsychological impairment were observed in the current study.[79] This study provides yet another example of hepatic metabolic reprogramming in response to persistent AhR activation by TCDD. Previous studies have shown that TCDD disrupts pathways associated with glucose and lipid metabolism, iron homeostasis, fibrosis, bile acid metabolism and enterohepatic circulation, and OCM.[21,23,24,26,32,38] The diurnal regulation of hepatic metabolism and the gut microbiome are also dose-dependently altered by TCDD.[33,80] The lack of TCDD hepatotoxicity in null mice suggests that these effects are likely mediated by the AhR.[81] Consequently, the prevailing hypothesis regarding the toxicity of TCDD and related compounds has focused on AhR-mediated changes in gene expression. Accumulating evidence suggests that persistent metabolic reprogramming may also be a significant contributing factor following the identification of accumulating toxic metabolic intermediates such as secondary bile acids, dicarboxylic acids, and acrylyl-CoA as well as alterations in the levels of key regulatory metabolites including ROS, acetyl-CoA, and *S*-adenosylmethionine (SAM). The results of this study suggest that disruptions in cysteine and H_2S levels following repression of the transsulfuration pathway may also be a contributing factor in the hepatotoxicity of TCDD and related compounds.

In response to increased oxidative stress and levels of toxic metabolic intermediates, cysteine import is increased via the induction of the cystine/glutamate Xc^- antiporter to support GSH biosynthesis due to the repression of the transsulfuration pathway. However, the persistent activation of AhR by TCDD is a constant strain on antioxidant defenses as is evident by the reduced GSH/GSSG ratio and increased ophthalmic acid levels. Another unintended consequence is the extended period of increased metabolic enzyme S-glutathionylation that may affect the flux of critical pathways required to sustain viability such as glycolysis, mitochondrial solute import, amino acid metabolism, the Krebs cycle, oxidative phosphorylation, and fatty acid oxidation.[82] Although the initial GSH defensive response protects susceptible sulfhydryl groups within critical metabolic enzymes from irreversible oxidation and degradation, prolonged S-glutathionylation may compromise cellular bioenergetics due to the metabolic reprogramming of glycolysis and the repression of β-oxidation.[31,83] Collectively, this suggests that the hepatotoxicity and the progression of steatosis to steatohepatitis with fibrosis elicited by TCDD and related compounds goes beyond AhR-mediated gene expression but also involves the cumulative burden of multiple hits as a result of metabolic disruption that produces toxic intermediates and compromises cellular bioenergetics.

■ ASSOCIATED CONTENT

Data Availability Statement

RNA-Seq and AhR CHIP-Seq data are available through Gene Expression Omnibus (GSE109863, GSE87519, GSE119780, GSE97634, GSE87542, GSE90097, GSE171942, GSE89430, GSE171941).

Supporting Information

The Supporting Information is available free of charge at https://pubs.acs.org/doi/10.1021/acs.chemrestox.3c00017.

Images of western blots used for analysis (Figure S1); expression of *Slc7a11* in hepatocytes from male mice following isolation and plating (Figure S2); effect of TCDD on hepatic *Slc1a4*, *Slc1a5*, and *Slc7a11* expression (Figure S3); cystine/glutamate Xc^- antiporter protein levels following TCDD treatment (Figure S4); effect of TCDD on Xc^- protein level−WES row data (Figure S5); MRM transitions of MS method (Table S1); and accurate masses and retention times of compounds analyzed on the quadrupole time of flight (Table S2) (PDF)

■ AUTHOR INFORMATION

Corresponding Author

Timothy R. Zacharewski − *Biochemistry & Molecular Biology and Institute for Integrative Toxicology, Michigan State University, East Lansing, Michigan 48824, United States;* orcid.org/0000-0002-3662-7919; Email: tzachare@msu.edu

Authors

Karina Orlowska − *Biochemistry & Molecular Biology and Institute for Integrative Toxicology, Michigan State University, East Lansing, Michigan 48824, United States*

Russ R. Fling − *Institute for Integrative Toxicology and Microbiology & Molecular Genetics, Michigan State University, East Lansing, Michigan 48824, United States*

https://doi.org/10.1021/acs.chemrestox.3c00017
Chem. Res. Toxicol. 2023, 36, 900−915

Rance Nault − *Biochemistry & Molecular Biology and Institute for Integrative Toxicology, Michigan State University, East Lansing, Michigan 48824, United States;* orcid.org/0000-0002-6822-4962

Anthony L. Schilmiller − *Mass Spectrometry and Metabolomics Core, Michigan State University, East Lansing, Michigan 48824, United States*

Complete contact information is available at: https://pubs.acs.org/10.1021/acs.chemrestox.3c00017

Author Contributions

Conception and design of the study: T.R.Z., R.N.; acquisition of data: K.O., R.R.F., R.N.; analysis and interpretation of data: T.R.Z., K.O., R.R.F., R.N.; A.L.S.; drafting the article or revising it critically for important intellectual content: T.R.Z., K.O., R.R.F., R.N.; A.L.S.; final approval of the version to be submitted: T.R.Z., K.O., R.R.F., R.N.; A.L.S. CRediT: **Karina Orlowska** investigation, methodology, visualization, writing-original draft, writing-review & editing; **Russ R Fling** investigation, methodology, writing-original draft, writing-review & editing; **Rance Nault** funding acquisition, investigation, methodology, software, writing-review & editing; **Anthony L. Schilmiller** methodology, writing-review & editing; **Timothy R. Zacharewski** conceptualization, funding acquisition, supervision, writing-original draft, writing-review & editing.

Notes

The authors declare no competing financial interest.

■ ACKNOWLEDGMENTS

This project was supported by the National Institute of Environmental Health Sciences Superfund Research Program [NIEHS SRP P42ES004911] and R01ES029541 to T.R.Z. T.R.Z. was partially supported by AgBioResearch at Michigan State University. R.R.F. was supported by NIEHS Multidisciplinary Training in Environmental Toxicology [T32ES007255].

■ REFERENCES

(1) Aquilano, K.; Baldelli, S.; Ciriolo, M. R. Glutathione: New Roles in Redox Signalling for an Old Antioxidant. *Front. Pharmacol.* **2014**, No. 196.

(2) Lu, S. C. Glutathione Synthesis. *Biochim. Biophys. Acta, Gen. Subj.* **2013**, *1830*, 3143−3153.

(3) Lu, S. C. Regulation of Glutathione Synthesis Shelly. *Mol. Aspects Med.* **2009**, *30*, 42−59.

(4) Ballatori, N.; Krance, S. M.; Notenboom, S.; Shi, S.; Tieu, K.; Hammond, C. L. Glutathione Dysregulation and the Etiology and Progression of Human Diseases. *Biol. Chem.* **2009**, *390*, 191−214.

(5) Dalle-donne, I.; Rossi, R.; Giustarini, D.; Colombo, R.; Milzani, A. S-Glutathionylation in Protein Redox Regulation. *Free Radical Biol. Med.* **2007**, *43*, 883−898.

(6) Jones, D. P. Redefining Oxidative Stress. *Antioxid. Redox Signaling* **2006**, *8*, 1865−1879.

(7) Lu, S. C. Regulation of Hepatic Glutathione Synthesis: Current Concepts and Controversies. *FASEB J.* **1999**, *13*, 1169−1183.

(8) Mosharov, E.; Cranford, M. R.; Banerjee, R. The Quantitatively Important Relationship between Homocysteine Metabolism and Glutathione Synthesis by the Transsulfuration Pathway and Its Regulation by Redox Changes. *Biochemistry* **2000**, *39*, 13005−13011.

(9) Banerjee, R.; Zou, C. Redox Regulation and Reaction Mechanism of Human Cystathionine- b -Synthase: A PLP-Dependent Hemesensor Protein. *Arch. Biochem. Biophys.* **2005**, *433*, 144−156.

(10) Mistry, R. K.; Brewer, A. C. Redox-Dependent Regulation of Sulfur Metabolism in Biomolecules: Implications for Cardiovascular Health. *Antioxid. Redox Signaling* **2019**, *30*, 972−991.

(11) Sbodio, J. I.; Snyder, S.; Paul, B. D. Regulators of the Transsulfuration Pathway. *Br. J. Pharmacol.* **2019**, *176*, 583−593.

(12) Werge, M. P.; Mccann, A.; Galsgaard, E. D.; Holst, D.; Bugge, A.; Albrechtsen, N. J. W.; Gluud, L. L. The Role of the Transsulfuration Pathway in Non-Alcoholic Fatty Liver Disease. *J. Clin. Med.* **2021**, *10*, No. 1081.

(13) Nebert, D. W.; Roe, A. L.; Dieter, M. Z.; Solis, W. A.; Yang, Y.; Dalton, T. P. Role of the Aromatic Hydrocarbon Receptor and [Ah] Gene Battery in the Oxidative Stress Response, Cell Cycle Control, and Apoptosis. *Biochem. Pharmacol.* **2000**, *59*, 65−85.

(14) Sugihara, K.; Kitamura, S.; Yamada, T.; Ohta, S.; Yamashita, K.; Yasuda, M.; Fujii-kuriyama, Y. Aryl Hydrocarbon Receptor (AhR) -Mediated Induction of Xanthine Oxidase/Xanthine Dehydrogenase Activity by 2, 3, 7, 8-Tetrachlorodibenzo- p -Dioxin. *Biochem. Biophys. Res. Commun.* **2001**, *281*, 1093−1099.

(15) Denison, M. S.; Faber, S. C. And Now for Something Completely Different: Diversity in Ligand-Dependent Activation of Ah Receptor Responses. *Curr. Opin. Toxicol.* **2017**, *2*, 124−131.

(16) Avilla, M. N.; Malecki, K. M. C.; Hahn, M. E.; Wilson, R. H.; Bradfield, C. A. The Ah Receptor: Adaptive Metabolism, Ligand Diversity, and the Xenokine Model. *Chem. Res. Toxicol.* **2020**, *33*, 860−879.

(17) Dere, E.; Lo, R.; Celius, T.; Matthews, J.; Zacharewski, T. R. Integration of Genome-Wide Computation DRE Search, AhR ChIP-Chip and Gene Expression Analyses of TCDD-Elicited Responses in the Mouse Liver. *BMC Genomics* **2011**, *12*, No. 365.

(18) Dalton, T. P.; Puga, A.; Shertzer, H. G. Induction of Cellular Oxidative Stress by Aryl Hydrocarbon Receptor Activation. *Chem.−Biol. Interact.* **2002**, *141*, 77−95.

(19) Rolo, A. P.; Teodoro, J. S.; Palmeira, C. M. Role of Oxidative Stress in the Pathogenesis of Nonalcoholic Steatohepatitis. *Free Radical Biol. Med.* **2012**, *52*, 59−69.

(20) Chen, Z.; Tian, R.; She, Z.; Cai, J.; Li, H. Free Radical Biology and Medicine Role of Oxidative Stress in the Pathogenesis of Nonalcoholic Fatty Liver Disease. *Free Radical Biol. Med.* **2020**, *152*, 116−141.

(21) Fader, K. A.; Nault, R.; Zhang, C.; Kumagai, K.; Harkema, J. R.; Zacharewski, T. R. 2,3,7,8-Tetrachlorodibenzo-p-Dioxin (TCDD)-Elicited Effects on Bile Acid Homeostasis: Alterations in Biosynthesis, Enterohepatic Circulation, and Microbial Metabolism. *Sci. Rep.* **2017**, *7*, No. 5921.

(22) Nault, R.; Colbry, D.; Brandenberger, C.; Harkema, J. R.; Zacharewski, T. R. Development of a Computational High-Throughput Tool for the Quantitative Examination of Dose-Dependent Histological Features. *Toxicol. Pathol.* **2015**, *43*, 366−375.

(23) Nault, R.; Fader, K. A.; Kopec, A. K.; Harkema, J. R.; Zacharewski, T. R.; Luyendyk, J. P. Coagulation-Driven Hepatic Fibrosis Requires Protease Activated Receptor-1 (PAR-1) in a Mouse Model of TCDD-Elicited Steatohepatitis. *Toxicol. Sci.* **2016**, *154*, 381−391.

(24) Nault, R.; Fader, K. A.; Kirby, M. P.; Ahmed, S.; Matthews, J.; Jones, A. D.; Lunt, S. Y.; Zacharewski, T. R. Pyruvate Kinase Isoform Switching and Hepatic Metabolic Reprogramming by the Environmental. *Toxicol. Sci.* **2016**, *149*, 358−371.

(25) Anastasiou, D.; Poulogiannis, G.; Asara, J. M.; Boxer, M. B.; Jiang, J.; Shen, M.; Bellinger, G.; Sasaki, A. T.; Locasale, J. W.; Auld, D. S.; Thomas, C. J.; Heiden, M. G. V.; Cantley, L. C. Inhibition of Pyruvate Kinase M2 by Reactive Oxygen Species Contributes to Cellular Antioxidant Responses. *Science* **2011**, *334*, 1278−1283.

(26) Fling, R. R.; Doskey, C. M.; Fader, K. A.; Nault, R.; Zacharewski, T. R. 2, 3, 7,8 -Tetrachlorodibenzo- P-dioxin (TCDD) Dysregulates Hepatic One Carbon Metabolism during the Progression of Steatosis to Steatohepatitis with Fibrosis in Mice. *Sci. Rep.* **2020**, No. 14831.

(27) Sorg, O.; Zennegg, M.; Schmid, P.; Fedosyuk, R.; Valikhnovskyi, R.; Gaide, O.; Kniazevych, V.; Saurat, J. H. 2,3,7,8-

Tetrachlorodibenzo-p-Dioxin (TCDD) Poisoning in Victor Yushchenko: Identification and Measurement of TCDD Metabolites. *Lancet* **2009**, *374*, 1179−1185.
(28) Wolfe, W. H.; Michalek, J. E.; Miner, J. C.; Pirkle, J. L.; Caudill, S. P.; Patterson, D. G.; Needham, L. L. Determinants of TCDD Half-Life in Veterans of Operation Ranch Hand. *J. Toxicol. Environ. Health* **1994**, *41*, 481−488.
(29) Gasiewicz, T.; Geiger, L.; Rucci, G.; Neal, R. Distribution, Excretion, and Metabolism of 2,3,7,8-Tetrachlorodibenzo-p-Dioxin in C57BL/6J, DBA/2J, and B6D2F1/J Mice. *Drug Metab. Dispos.* **1983**, *11*, 397−403.
(30) Angrish, M. M.; Dominici, C. Y.; Zacharewski, T. R. TCDD-Elicited Effects on Liver, Serum, and Adipose Lipid Composition in C57BL/6 Mice. *Toxicol. Sci.* **2013**, *131*, 108−115.
(31) Nault, R.; Fader, K. A.; Ammendolia, D. A.; Dornbos, P.; Potter, D.; Sharratt, B.; Kumagai, K.; Harkema, J. R.; Lunt, S. Y.; Matthews, J.; Zacharewski, T. Dose-Dependent Metabolic Reprogramming and Differential Gene Expression in TCDD-Elicited Hepatic Fibrosis. *Toxicol. Sci.* **2016**, *154*, 253−266.
(32) Nault, R.; Fader, K. A.; Lydic, T. A.; Zacharewski, T. R. Lipidomic Evaluation of Aryl Hydrocarbon Receptor-Mediated Hepatic Steatosis in Male and Female Mice Elicited by 2,3,7,8-Tetrachlorodibenzo-p-Dioxin. *Chem. Res. Toxicol.* **2017**, *30*, 1060−1075.
(33) Fader, K. A.; Nault, R.; Doskey, C. M.; Fling, R. R.; Zacharewski, T. R. 2,3,7,8-Tetrachlorodibenzo-p-Dioxin Abolishes Circadian Regulation of Hepatic Metabolic Activity in Mice. *Sci. Rep.* **2019**, *9*, No. 6514.
(34) Lee, J. H.; Wada, T.; Febbraio, M.; He, J.; Matsubara, T.; Lee, M. J.; Gonzalez, F. J.; Xie, W. A Novel Role for the Dioxin Receptor in Fatty Acid Metabolism and Hepatic Steatosis. *Gastroenterology* **2010**, *139*, 653−663.
(35) Gil, A.; van der Pol, A.; van der Meer, P.; Bischoff, R. LC-MS Analysis of Key Components of the Glutathione Cycle in Tissues and Body Fluids from Mice with Myocardial Infarction. *J. Pharm. Biomed. Anal.* **2018**, *160*, 289−296.
(36) Liu, R.; Bi, K.; Jia, Y.; Wang, Q.; Yin, R.; Li, Q. Determination of Polyamines in Human Plasma by High-Performance Liquid Chromatography Coupled with Q-TOF Mass Spectrometry. *J. Mass Spectrom.* **2012**, *47*, 1341−1346.
(37) Eckel, J. E.; Gennings, C.; Chinchilli, V. M.; Burgoon, L. D.; Zacharewski, T. R. Empirical Bayes Gene Screening Tool for Time-Course or Dose-Response Microarray Data. *J. Biopharm. Stat.* **2004**, *14*, 647−670.
(38) Fader, K. K. A.; Nault, R.; Kirby, M. M. P.; Markous, G.; Matthews, J.; Zacharewski, T. R. Convergence of Hepcidin Deficiency, Systemic Iron Overloading, Heme Accumulation, and REV-ERBα/β Activation in Aryl Hydrocarbon Receptor-Elicited Hepatotoxicity. *Toxicol. Appl. Pharmacol.* **2017**, *321*, 1−17.
(39) Nault, R.; Doskey, C. M.; Fader, K. A.; Rockwell, C. E.; Zacharewski, T. Comparison of Hepatic NRF2 and Aryl Hydrocarbon Receptor Binding in 2,3,7,8-Tetrachlorodibenzo-p-Dioxin−Treated Mice Demonstrates NRF2-Independent PKM2 Induction. *Mol. Pharmacol.* **2018**, *94*, 876−884.
(40) Sullivan, B. P.; Kopec, A. K.; Joshi, N.; Cline, H.; Brown, J. A.; Bishop, S. C.; Kassel, K. M.; Rockwell, C.; Mackman, N.; Luyendyk, J. P. Hepatocyte Tissue Factor Activates the Coagulation Cascade in Mice. *Blood* **2013**, *121*, 1868−1874.
(41) Olsavsky Goyak, K. M.; Laurenzana, E.; Omiecinski, C.Hepatocyte Differentiation. In *Hepatocytes*; Maurel, P., Ed.; Methods in Molecular Biology; Humana Press, 2010; Vol. *640*, pp 115−138.
(42) Mizuguchi, T.; Hui, T.; Palm, K.; Sugiyama, N.; Mitaka, T.; Demetriou, A. A.; Rozga, J. Enhanced Proliferation and Differentiation of Rat Hepatocytes Cultured with Bone Marrow Stromal Cells. *J. Cell. Physiol.* **2001**, *189*, 106−119.
(43) Fader, K. A.; Nault, R.; Ammendolia, D. A.; Harkema, J. R.; Williams, K. J.; Crawford, R. B.; Kaminski, N. E.; Potter, D.; Sharratt, B.; Zacharewski, T. R. Metabolism and Depletes Immune Cell Populations in the Jejunum of C57BL/6 Mice. *Toxicol. Sci.* **2015**, *148*, 567−580.
(44) Orlowska, K.; Fling, R. R.; Nault, R.; Sink, W. J.; Schilmiller, A. L.; Zacharewski, T. Dioxin-Elicited Decrease in Cobalamin Redirects Propionyl-CoA Metabolism to the β−Oxidation-like Pathway Resulting in Acrylyl-CoA Conjugate Buildup. *J. Biol. Chem.* **2022**, *298*, No. 102301.
(45) Finkelstein, J. D. Metabolic Regulatory Properties of S-Adenosylmethionine and S-Adenosylhomocysteine. *Clin. Chem. Lab. Med.* **2007**, *45*, 1694−1699.
(46) Mandal, P. K.; Seiler, A.; Perisic, T.; Ko, P.; Canak, A. B.; Fo, H.; Weiss, N.; Kremmer, E.; Lieberman, M. W.; Bannai, S.; Kuhlencordt, P.; Sato, H.; Bornkamm, G. W.; Conrad, M. System Xc- and Thioredoxin Reductase 1 Cooperatively Rescue Glutathione Deficiency. *J. Biol. Chem.* **2010**, *285*, 22244−22253.
(47) Sasaki, H.; Sato, H.; Kuriyama-matsumura, K.; Sato, K.; Maebara, K.; Wang, H.; Tamba, M.; Itoh, K.; Yamamoto, M.; Bannai, S. Electrophile Response Element-Mediated Induction of the Cystine / Glutamate Exchange Transporter Gene Expression. *J. Biol. Chem.* **2002**, *277*, 44765−44771.
(48) Pader, I.; Sengupta, R.; Cebula, M.; Xu, J.; Lundberg, J. O.; Holmgren, A.; et al. Thioredoxin-Related Protein of 14 KDa Is an Efficient L-Cystine Reductase and S-Denitrosylase. *Proc. Natl. Acad. Sci. U.S.A.* **2014**, *111*, 6964−6969.
(49) Soga, T.; Baran, R.; Suematsu, M.; Ueno, Y.; Ikeda, S.; Sakurakawa, T.; Kakazu, Y.; Ishikawa, T.; Robert, M.; Nishioka, T.; Tomita, M. Differential Metabolomics Reveals Ophthalmic Acid as an Oxidative Stress Biomarker Indicating Hepatic Glutathione Consumption. *J. Biol. Chem.* **2006**, *281*, 16768−16776.
(50) Singhal, S. S.; Yadav, S.; Roth, C.; Singhal, J. RLIP76: A Novel Glutathione-Conjugate and Multi-Drug Transporter. *Biochem. Pharmacol.* **2009**, *77*, 761−769.
(51) Lash, L. H. Role of Glutathione Transport Processes in Kidney Function. *Toxicol. Appl. Pharmacol.* **2005**, *204*, 329−342.
(52) Bachhawat, A. K.; Thakur, A.; Kaur, J.; Zulkifli, M. Glutathione Transporters. *Biochim. Biophys. Acta, Gen. Subj.* **2013**, *1830*, 3154−3164.
(53) Irino, Y.; Toh, R.; Nagao, M.; Mori, T.; Honjo, T.; Shinohara, M.; Tsuda, S.; Nakajima, H.; Satomi-Kobayashi, S.; Shinke, T.; Tanaka, H.; Ishida, T.; Miyata, O.; Hirata, K. I. 2-Aminobutyric Acid Modulates Glutathione Homeostasis in the Myocardium. *Sci. Rep.* **2016**, *6*, No. 36749.
(54) McCourt, J. A.; Duggleby, R. G. Acetohydroxyacid Synthase and Its Role in the Biosynthetic Pathway for Branched-Chain Amino Acids. *Amino Acids* **2006**, *31*, 173−210.
(55) Steele, R. D.; Weber, H.; Patterson, J. I. Characterization of α-Ketobutyrate Metabolism in Rat Tissues: Effects of Dietary Protein and Fasting. *J. Nutr.* **1984**, *114*, 701−710.
(56) Lee, J.; Kang, E. S.; Kobayashi, S.; Homma, T.; Sato, H.; Seo, H. G.; Fujii, J. The Viability of Primary Hepatocytes Is Maintained under a Low Cysteine-Glutathione Redox State with a Marked Elevation in Ophthalmic Acid Production. *Exp. Cell Res.* **2017**, *361*, 178−191.
(57) Gout, P. W.; Buckley, A. R.; Simms, C. R.; Bruchovsky, N. Sulfasalazine, a Potent Suppressor of Lymphoma Growth by Inhibition of the x χ Cystine Transporter: A New Action for an Old Drug. *Leukemia* **2001**, *15*, 1633−1640.
(58) Manevich, Y.; Feinstein, S. I.; Fisher, A. B. Activation of the Antioxidant Enzyme 1-CYS Peroxiredoxin Requires Glutathionylation Mediated by Heterodimerization with GST. *Proc. Natl. Acad. Sci. U.S.A.* **2004**, *101*, 3780−3785.
(59) Townsend, D.; Manevich, Y.; He, L.; Hutchens, S.; Pazoles, C. J.; Tew, K. D. Novel Role for Glutathione S-Transferase π Regulator of Protein S-Glutathionylation following Oxidative and Nitrosative Stress. *J. Biol. Chem.* **2009**, *284*, 436−445.
(60) McGarry, D. J.; Chen, W.; Chakravarty, P.; Lamont, D. L.; Wolf, C. R.; Henderson, C. J. Proteome-Wide Identification and Quantification of S-Glutathionylation Targets in Mouse Liver. *Biochem. J.* **2015**, *469*, 25−32.

https://doi.org/10.1021/acs.chemrestox.3c00017
Chem. Res. Toxicol. 2023, 36, 900−915

(61) Matsui, R.; Ferran, B.; Oh, A.; Croteau, D.; Shao, D.; Han, J.; Pimentel, D. R.; Bachschmid, M. M. Redox Regulation via Glutaredoxin-1 and Protein S -Glutathionylation. *Antioxid. Redox Signaling* **2020**, *32*, 677−700.
(62) Jung, C.-H.; Thomas, J. A. S-Glutathiolated Hepatocyte Proteins and Insulin Disulfides as Substrates for Reduction by Glutaredoxin, Thioredoxin, Protein Disulfide Isomerase, and Glutathione. *Arch. Biochem. Biophys.* **1996**, *335*, 61−72.
(63) Findlay, V. J.; Townsend, D. M.; Morris, T. E.; Fraser, J. P.; He, L.; Tew, K. D. A Novel Role for Human Sulfiredoxin in the Reversal of Glutathionylation. *Cancer Res.* **2006**, *66*, 6800−6807.
(64) Holmgren, A.; Johansson, C.; Berndt, C.; Lönn, M.; Hudemann, C.; Lillig, C. H. Thiol Redox Control via Thioredoxin and Glutaredoxin Systems. *Biochem. Soc. Trans.* **2005**, *33*, 1375−1377.
(65) Ogata, F. T.; Branco, V.; Vale, F. F.; Coppo, L. Redox Biology Glutaredoxin: Discovery, Redox Defense and Much More. *Redox Biol.* **2021**, *43*, No. 101975.
(66) Yeager, R. L.; Reisman, S. A.; Aleksunes, L. M.; Klaassen, C. D. Introducing the '"TCDD-Inducible AhR-Nrf2 Gene Battery."'. *Toxicol. Sci.* **2009**, *111*, 238−246.
(67) Prudova, A.; Bauman, Z.; Braun, A.; Vitvitsky, V.; Lu, S. C.; Banerjee, R. S-Adenosylmethionine Stabilizes Cystathionine β-Synthase and Modulates Redox Capacity. *Proc. Natl. Acad. Sci. U.S.A.* **2006**, *103*, 6489−6494.
(68) Orlowska, K.; Fling, R. R.; Nault, R.; Zacharewski, T.*2,3,7,8-Tetrachlorodibenzo-p-dioxin Elicited Decreases in Cobalamin Inhibits Methylmalonyl-CoA Mutase Activity Redirecting Propionyl-CoA Metabolism to the β−Oxidation-like Pathway Resulting in Hepatic Accumulation of the Toxic Intermediate Acrylyl-CoA*; bioRxiv, 2021
(69) Zuhra, K.; Tomé, C. S.; Forte, E.; Vicente, J. B.; Giuffrè, A. The Multifaceted Roles of Sulfane Sulfur Species in Cancer-Associated Processes. *Biochim. Biophys. Acta, Bioenerg.* **2021**, *1862*, No. 148338.
(70) Wei, W.; Wang, C.; Yi, J.; et al. The Content of Hydrogen Sulfide in Plasma of Cirrhosis Rats Combined with Portal Hypertension and the Correlation with Indexes of Liver Function and Liver Fibrosis. *Exp. Ther. Med.* **2017**, *14*, 5022−5026.
(71) Tan, G.; Pan, S.; Li, J.; Dong, X.; Kang, K.; Zhao, M.; Jiang, X.; Kanwar, J. R.; Qiao, H.; Jiang, H.; Sun, X. Hydrogen Sulfide Attenuates Carbon Tetrachloride-Induced Hepatotoxicity, Liver Cirrhosis and Portal Hypertension in Rats. *PLoS One* **2011**, *6*, No. e25943.
(72) Peh, M. T.; Anwar, A. B.; Ng, D. S. W.; Shirhan Bin Mohamed Atan, M.; Kumar, S. D.; Moore, P. K. Effect of Feeding a High Fat Diet on Hydrogen Sulfide (H2S) Metabolism in the Mouse. *Nitric Oxide* **2014**, *41*, 138−145.
(73) Wu, D.; Zheng, N.; Qi, K.; Cheng, H.; Sun, Z.; Gao, B.; Zhang, Y.; Pang, W.; Huangfu, C.; Ji, S.; Xue, M.; Ji, A.; Li, Y. Exogenous Hydrogen Sulfide Mitigates the Fatty Liver in Obese Mice through Improving Lipid Metabolism and Antioxidant Potential. *Med. Gas Res.* **2015**, *5*, No. 1.
(74) Ballatori, N.; Krance, S. M.; Marchan, R.; Hammond, C. L. Plasma Membrane Glutathione Transporters and Their Roles in Cell Physiology and Pathophysiology. *Mol. Aspects Med.* **2009**, *30*, 13−28.
(75) Oestreicher, J.; Morgan, B. Glutathione: Subcellular Distribution and Membrane Transport. *Biochem. Cell Biol.* **2019**, *97*, 270−289.
(76) Gao, X. H.; Li, L.; Parisien, M.; Wu, J.; Bederman, I.; Gao, Z.; Krokowski, D.; Chirieleison, S. M.; Abbott, D.; Wang, B.; Arvan, P.; Cameron, M.; Chance, M.; Willard, B.; Hatzoglou, M. Discovery of a Redox Thiol Switch: Implications for Cellular Energy Metabolism. *Mol. Cell. Proteomics* **2020**, *19*, 852−870.
(77) Zhang, J.; Ye, Z. w.; Singh, S.; Townsend, D. M.; Tew, K. D. An Evolving Understanding of the S-Glutathionylation Cycle in Pathways of Redox Regulation. *Free Radical Biol. Med.* **2018**, *120*, 204−216.
(78) Musaogullari, A.; Chai, Y. C. Redox Regulation by Protein S-Glutathionylation: From Molecular Mechanisms to Implications in Health and Disease. *Int. J. Mol. Sci.* **2020**, *21*, No. 8113.
(79) Pelclová, D.; Urban, P.; Preiss, J.; Lukäs, E.; Fenclovä, Z.; Navrätil, T.; Dubskä, Z.; Senholdovä, Z. Adverse Health Effects in Humans Exposed to 2,3,7,8-Tetrachlorodibenzo-p-Dioxin (TCDD). *Rev. Environ. Health* **2006**, *21*, 119−138.
(80) Nichols, R. G.; Zhang, J.; Cai, J.; Murray, I. A.; Koo, I.; Smith, P. B.; Perdew, G. H.; Patterson, A. D. Metatranscriptomic Analysis of the Mouse Gut Microbiome Response to the Persistent Organic Pollutant 2,3,7,8-Tetrachlorodibenzofuran. *Metabolites* **2020**, *10*, No. 1.
(81) Fernandez-Salguero, P.; Hilbert, D.; Rudikoff, S.; Ward, J.; Gonzalez, F. Aryl-hydrocarbon Receptor-Deficient Mice Are Resistant to 2,3,7,8-Tetrachlorodibenzo-p-dioxin-Induced Toxicity. *Toxicol. Appl. Pharmacol.* **1996**, *140*, 173−179.
(82) Mailloux, R. J. Protein S-Glutathionylation Reactions as a Global Inhibitor of Cell Metabolism for the Desensitization of Hydrogen Peroxide Signals. *Redox Biol.* **2020**, *32*, No. 101472.
(83) Cholico, G. N.; Fling, R. R.; Zacharewski, N. A.; Fader, K. A.; Nault, R.; Zacharewski, T. Thioesterase Induction by 2,3,7,8-Tetrachlorodibenzo-p-Dioxin Results in a Futile Cycle That Inhibits Hepatic β-Oxidation. *Sci. Rep.* **2021**, *11*, No. 15689.

https://doi.org/10.1021/acs.chemrestox.3c00017
Chem. Res. Toxicol. 2023, 36, 900−915